Experimental and Numerical Analysis of Angular Error in Taper Cutting using Wire Electrical Discharge Machining

Surinarayana Cherukuri

Department of Mechanical Engineering
National Institute of Technology Rourkela

Experimental and Numerical Analysis of Angular Error in Taper Cutting using Wire Electrical Discharge Machining

Thesis submitted in partial fulfillment

Of the requirements of the degree of

Masters of Technology

in

Mechanical Engineering

by

Surinarayana Cherukuri

(214ME2548)

Under the supervision of

Dr. Siba Sankar Mahapatra

MAY 2016

DEPARTMENT OF MECHANICAL ENGINEERING

NATIONAL INSTITUTE OF TECHNOLOGY, ROURKELA

Department of Mechanical Engineering

National Institute of Technology Rourkela

Prof. Siba Sankar Mahapatra

Professor

May 25, 2016

Supervisor's Certificate

This is to certify that the work presented in this dissertation entitled *Experimental and Numerical Analysis of Angular Error in Taper Cutting using Wire Electrical Discharge Machining* by *Surinarayana Cherukuri* Roll Number 214ME2548 is a record of original research carried out by him under my supervision and guidance in partial fulfillment of the requirements of the degree of *Master of Technology* in *Department of Mechanical Engineering*. Neither this dissertation nor any part of it has been submitted for any degree or diploma to any institute or university in India or abroad.

……

Siba Sankar Mahapatra

Professor

Dedicated to my Family, Guide and well-wishers...

Declaration of Originality

I, Surinarayana Cherukuri, roll no. 214ME2548 hereby declare that this dissertation entitled "*Experimental and Numerical Analysis of Angular Error in Taper Cutting using Wire Electrical Discharge Machining*" represents my original work carried out as a postgraduate student of NIT Rourkela and, to the best of my knowledge, it contains no material previously published or written by another person, nor any material presented for the award of any other degree or diploma of NIT Rourkela or any other institution. Any contribution made to this research by others, with whom I have worked at NIT Rourkela or elsewhere, is explicitly acknowledged in the dissertation. Works of other authors cited in this dissertation have been duly acknowledged under the section "Bibliography". I have also submitted my original research records to the scrutiny committee for evaluation of my dissertation.

I am fully aware that in case of any non-compliance detected in future, the Senate of NIT Rourkela may withdraw the degree awarded to me on the basis of the present dissertation.

May 25, 2016

NIT Rourkela **Surinarayana Cherukuri**

Acknowledgements

I express my deep sense of gratitude and indebtedness to my project supervisor **Prof. Siba Sankar Mahapatr**a, HEAD of the Department of Mechanical Engineering for providing precious guidance, inspiring discussions, and constant supervision throughout the course of this work. His timely help, constructive criticism, and conscientious efforts made it possible to present the work contained in the thesis. I am also indebted to Prof. Saurav Datta, for providing valuable departmental facilities.

Successful completion of work can never be one man's task. It requires hard work in right direction. There are many who have helped to make my experience as a student a rewarding one.

I am indebted to Dr. Bijaya Bijeta Nayak, **Suman Chatterjee**, and Shaibu Vb for support and care helped me overcome setbacks and stay focused on my research work. I wish to express my sincere thanks to **C.T.T.C** Bhubaneswar provided me with necessary facilities at various stages of this work. A very special thanks to **Chinmay Mohanty**, your words motivated me a lot.

I feel pleased and privileged to fulfill my parent's ambition and I am greatly indebted to them for bearing the inconvenience during my M.Tech course.

Surinarayana Cherukuri

Roll No: 214ME2548

Abstract

Today, there are far greater demands for higher precision in machining, use fewer tools and ease of operation. Wire electro discharge machining (WEDM) is one, mostly acceptable non-conventional machining processes, using fewer tools; ease machining and producing extreme accurate shapes in hard materials those using in the tooling industry where the extreme precision is required and complexly determines such as extrusion dies in wear-resistant materials, cutting dies, etc. Wire EDM Taper cutting took forward the generation of inclined ruled surfaces, and it is eminently more important in the manufacturing of tooling requiring draft angles. The required angle is reached by applying a relative moment between the lower guide and the upper guide. Deformation arises in the wire, during the machining of taper cutting using Wire EDM. Due to that deformation in the wire, effected to the ruled inclination of machined parts. Such circumstances cause a dimensional error, loss of tolerances and less precision that can prime to the rejection of high added value tooling. To predict the deformation of wire by considering contact mechanics, properties of wire, properties of the guide, boundary conditions, typically used in taper cutting operations, has been taking into the account. FEM is needed to reduce the experimental cost and lack of time consumption and to give a more common approach to the problem. Finite Element Model (FEM) has been used to find out the deformation occurs during wire EDM process by changing the wire parameters like wire tension, wire diameter, taper angle and wire length, which is generally considering in taper cutting. This result intends to give you better understanding shows that taper angle and wire length are the most effective parameters in taper cutting process. Taguchi's L_{16} orthogonal array is used to reduce the experimental runs. Traditional Taguchi approach is insufficient to solve a multi-response optimization problem. In order to overcome this limitation, utility theory has been implemented, to convert multi-responses into single

equivalent response called overall utility index. Both the results, FEM and experimental have been checked.

Keywords: - Wire Electrical discharge machining, taper cutting, deformation, angular error, Finite element model, utility theory

Contents

List of Figures

List of Tables

Chapter 1

Introduction

1.1 History

The beginning of EDM came during the Second World War when two Russian physicists B.R. and N.I. Lazarenko published their study on The Inversion of the Electric Discharge Wear Effect, Which related to the application of manufacturing technology of the capacity of electrical discharges, under controlled distribution, to remove metal.

EDM was being used at that time to remove broken taps and drills. The early “Tap-Busters” disintegrated taps with hand fed electrodes, burning a hole in the center of the tap or drill, leaving the remaining fragments that could be picked out. This saved workpieces and very expensive parts from being scrapped and having to be made over again.

This process opened the birth of Vertical EDM, also called: Sinker, Conventional, Ram, Plunge or Diesinker EDM’s. These machines were, and still are primarily used to make precision cavities in metal primarily for the mold industry.

1.2 Wire EDM

Wire EDM, in the late 1960s' it was introduced and has modernized the tool and die, mold, and metal working industries. In the last fifty years, probably the most exciting and diversified machine tool developed for this industry and has numerous advantages to offer. Wire Electrical discharge machining (WEDM) is one of the most likely used advanced controlled material removal processes by means of electric spark erosion. It can machine anything that is electrically conductive regardless of the hardness, from relatively common materials such as tool steel, aluminum, copper, and graphite, to exotic space-age alloys including Hastelloy, Waspaloy, Inconel, titanium, carbide, polycrystalline diamond compacts and conductive ceramics. The wire does not touch the workpiece, so there is no physical pressure imparted on the workpiece compared to grinding wheels and milling cutters. The amount of clamping pressure required to hold small, thin and fragile parts is minimal, preventing damage or distortion to the workpiece.

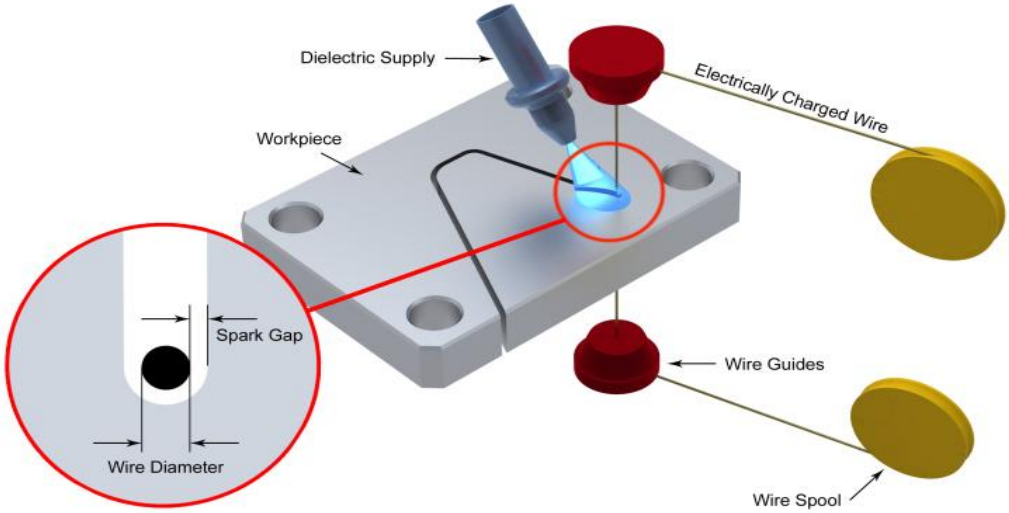

Figure 1-1 Wire electrical discharge machining working principle

Wire EDM also gives designers more latitude in designing dies, and management more control of manufacturing, since the machining is completed automatically. Parts that have complex geometry and tolerances don't require relying on different multiple or skill levels equipment. Substantial increases in productivity are achieved since the machining is intended, allowing operators to do work in other areas. Most machines run overnight in a "lights-out" environment. Long jobs are cut overnight, or over the weekend, while shorter jobs are scheduled during the day. Most workpieces come off the machine as a finished part, without the need for secondary operations. It's a one-step process.

1.3 Working principle of Wire EDM

The working principle of EDM and WEDM is similar. Both the tool and the work materials are to be conductors of electricity. The tool and the work material are immersed in a dielectric medium. A series of discrete electric spark is used as the cutting tool to cut the workpiece to produce the finished part to the desired shape. Generally, the tool is connected to the negative (cathode) terminal of the generator and the workpiece is connected to positive (anode) terminal. The metal removal process is performed by applying a pulsating electric charge of high-frequency current through the electrode to the workpiece. This erodes very tiny pieces of metal from the workpiece at a controlled rate. The only difference in EDM

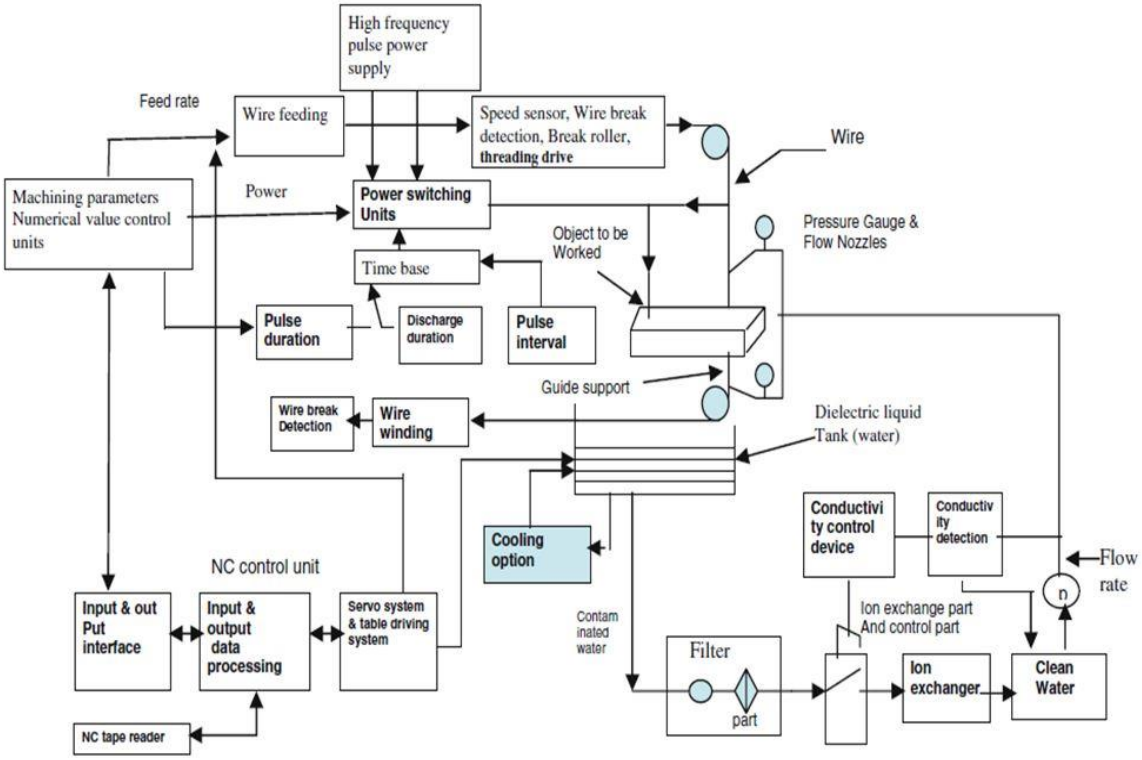

Figure 1-2 Block diagram of WEDM (Mahapatra et al., 2007)

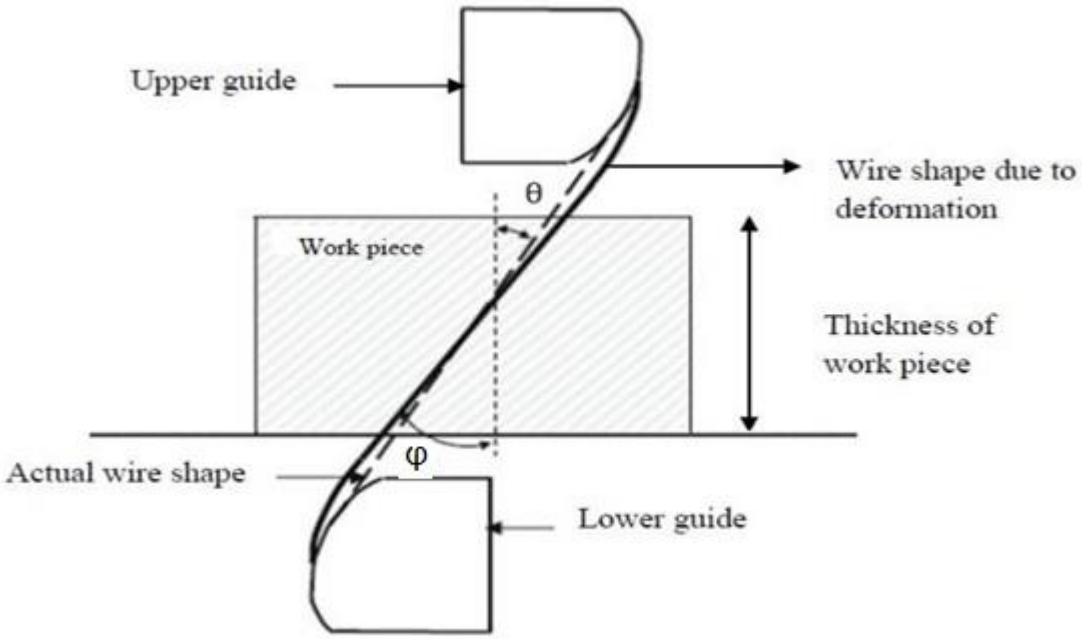

Figure 1-3 Schematic representation of deformation of wire in taper cutting of WEDM

and WEDM; in EDM machining specially shaped electrodes (usually made from graphite or copper) are require; only wire (Brass) is required in WEDM for machining. The required angle is reached by applying a relative moment between the lower guide and the upper guide.

1.4 Hard Wire and Soft Wire

When conventional machining processes cannot successfully cut high taper angles, wire EDM can. However, mold manufacturers using wire EDM technology face some challenges when cutting such angles, which can range from 10 to 45 degrees. Oftentimes, EDM machines have the axis movement necessary to achieve the desired angle, but the physical properties of the wire and related machine technology may not be adequate. Examining the wire's properties is useful in determining the right wire for achieving the best cut.

Hard wire is stronger, straighter and more resistant to breakage during cutting than soft wire. High tensile strength, harder wire can also better fight deflection during cutting, but a very hard wire with little elongation can cause vibrations during taper cutting as the wire travels between the upper and lower wire guides. In addition, hard wire's "memory" resists the truly programmed wire path during high taper cutting, which bends the wire and can lead to reduced accuracy, poor surface finish or wire breakage. This will leave intolerable marks on the workpiece and waste material and production time.

A better solution for cutting high tapers is soft wire. Low tensile strength, soft wire easily bends to follow the correct path determined by the CNC controller and provide more accurate cuts. However, soft-wire has less memory than hard wire and is prone to breakage in aggressive cutting conditions. It is also sensitive to the voltages and tension applied to it by the EDM machine during the Automatic Wire Feed (AWF) cutting cycle. If not handled properly, the result is a malformed wire tip that is curved and prevents the wire from being able to be inserted into the wire guides. In these instances, the machine is unable to thread or rethread the wire, so the erosion process is stopped and production time is lost. The operator is required to manually intervene before cutting can begin again.

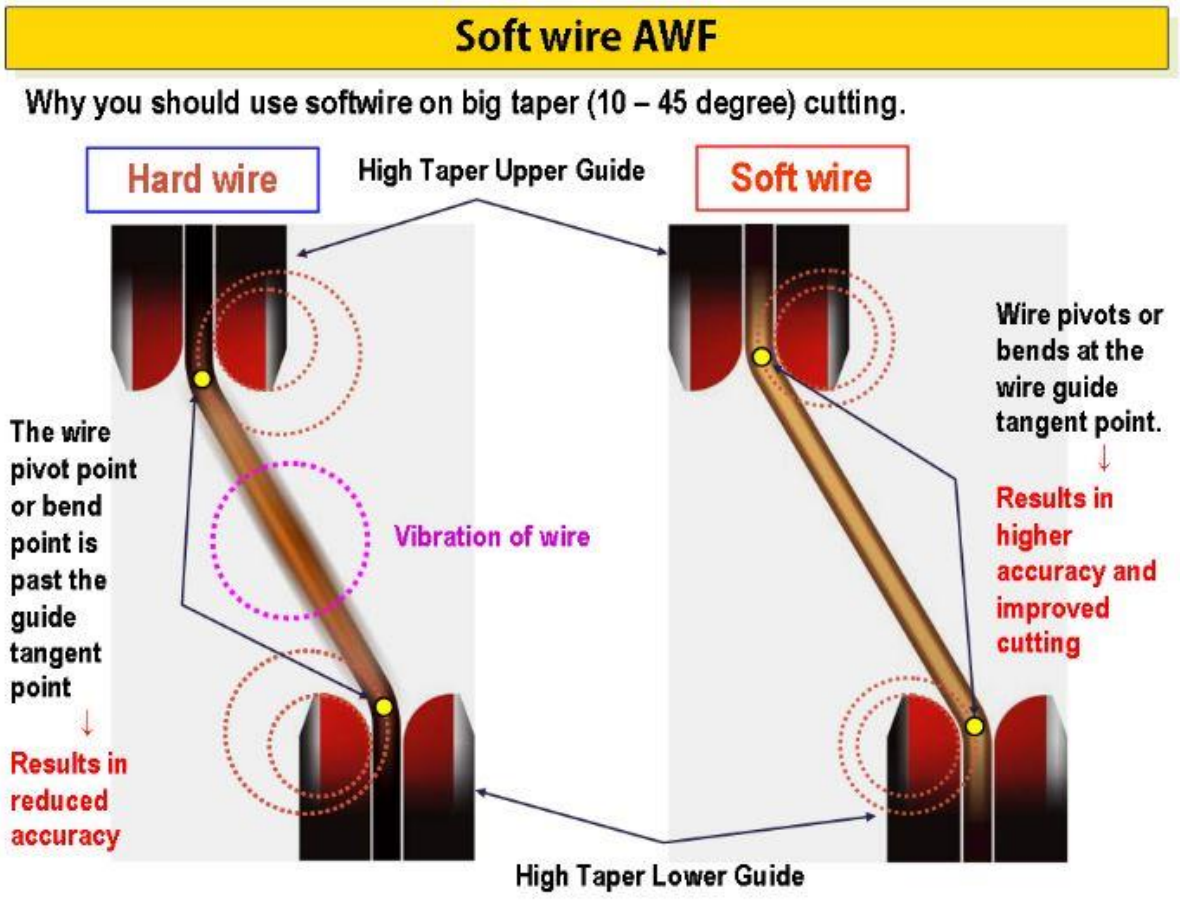

Figure 1-4 Difference between hard wire and soft wire [27]

1.4.1 Overcoming Obstacles: To overcome the challenges of soft wire threading, consider EDM equipment that provides improved wire processing during the AWF cutting cycle. Technology should include a way to precisely control the wire tension and energy used to cut the wire.

The ideal AWF situation is one where the wire heats and stretches until it breaks in two without melting. Using the ideal voltage needed to cut the wire and form a bullet point can enhance soft wire threading performance; improving the straightness of the wire and decreasing electrode wear (see Fig 3.1).

It is not just the hardness or softness of the wire that needs to be considered, however. Factors such as wire diameter, cutting and anneal tension, and voltage needs to be fine-tuned based on the wire selection in order to preserve the shape of the wire tip, minimize damage to the face and maximize straightness.

The small discharges used in wire EDM can result in electrode and wire tip damage, wire chip buildup and reduced AWF reliability. Some EDM machines offer an air blow system that directs cool air to the wire cut point. This keeps the wire tip as cool as possible and also prevents a molten tip from being produced during thermal wire cutting.

To optimize the threading cutting cycle, a relay on a timer is used to open an air solenoid to gently blow cool air onto the wire cutting electrode and keep the wire tip from heating up to a melting stage. This prohibits wire chip buildup, extends electrode life and provides reliable threading and cutting performance.

During the cutting phase, accurately controlling wire tension is critical (especially with soft wire), so an AWF system with a wire tension monitoring device that provides continuous observation is important. EDM systems that include an AC motor and encoder wire drive system working in tandem enable the tension motor and drive roller to communicate energy usage to the controller, and will allow the operator to better maintain wire tension throughout the cutting process.

There are also some measures the operator can take to improve cutting performance. When working with soft wire, it's important to use a die guide designed for large taper cutting, especially if you are going to skim cut the large tapers to improve surface finish and accuracy. These guides have a much larger support to help the wire transition through large angles. To ensure accuracy, also, use the features in the CNC that compensate for the changing position in Z-axis direction so that the taper angles are precise. Finally, if the cutting technology being used was developed for hard brass wire, the wire tension will have to be reduced on the rough cut. Opportunities and Applications

Technology developments in EDM have affected machining across many industries. The ability to accurately and efficiently machine taper cuts using soft wire has opened up new areas of opportunity for the technology. The more accurate and smooth the finish, the less additional, time-consuming, manual fitment and polishing is required by the mold maker.

1.5 Dielectric System

Wire EDM uses deionized water as the dielectric, that dielectric system includes the water reservoir, filtration system, deionization system, and water chiller unit. In EDM, as has been discussed earlier, material removal mainly occurs due to thermal evaporation and melting. As thermal processing is required to be carried out in the absence of oxygen so that the process can be controlled and oxidation avoided. Oxidation often leads to poor surface conductivity (electrical) of the workpiece hindering further machining. Hence, dielectric fluid should provide an oxygen free machining environment. Further, it should have enough strong dielectric resistance so that it does not breakdown electrically too easily but at the same time ionize when electrons collide with its molecule. Moreover, during sparking it should be thermally resistant as well.

Generally, kerosene and deionized water are used as the dielectric fluid in EDM. Tap water cannot be used as it ionizes too early and thus breakdown due to the presence of salts as impurities occur. Dielectric medium is generally flushed around the spark zone. It is also applied through the tool to achieve efficient removal of molten material.

During cutting, the dirty water is drained into the unfiltered side of the dielectric reservoir where the water is then pumped and filtered through a paper filter and returned to the clean side of the dielectric tank. Following filtration, the clean water is measured for conductivity, and if required passes through a vessel that contains a mixed bed of anion and cation beads. This mixed bed resin (the ion exchange unit) controls the resistivity of the water to set values automatically.

The clean water fills the clean side of the dielectric reservoir and proceeds to the cutting area. Used water is drained and returned to the unfiltered side of the dielectric reservoir to complete the cycle. A water chiller is provided as standard equipment to keep the dielectric, workpiece, worktable, control arms, and fixtures thermally stable. During the cutting process, the chips from the material that is being eroded gradually change the water conductivity level. Resistivity levels of the water are set according to the cutting requirements of the workpiece material being machined.

Chapter 2

Literature Survey

K.H. Ho et.al - Discussed on the various academic research areas involving the WEDM process. The research work carried out from the spin-off from the EDM process to the development of the WEDM. Machining process and productivity of the wire EDM are affected by the various factors of the optimization of the process parameters. Hybrid machining process (HMP) is combined the advantage of wire EDM with other machining techniques. Wire electro discharge grinding (WEDG) is one which is used for micro-machining of fine rods utilized in the electronic circuitry. WEDG employs a single wire guide to confine the wire tension within the discharge area between the rod and the front edge of the wire and to minimize the wire vibration. Therefore, it is possible to grind a rod that is as small as 5-micrometer diameter with high accuracy, good repeatability, and satisfactory straightness. HMPs needed to get better performance such as Cutting ratio (CR) and surface integrity. For example, ultrasonic vibration is applied to the wire electrode to improve the surface finishing and cutting ratio and to reduce residual stress on the machined surface. To produce good surface finished the part in a wide range replacing electrical discharge used in WEDG by wire electrochemical grinding. A rotary axis also added to WEDM to get higher material removal rate (MRR) and to enable the generation of free-form cylindrical geometries. A number of Process parameters play a crucial role in WEDM machining process. Minor changes in the process parameters can affect the machining performances which are most important aspects in the WEDM machining such as surface finish, accuracy, material removal rate, and cutting ratio. Control systems were explained, which are Fuzzy control system, wire inaccuracy adaptive control system (deals controlling wire breakage, wire lag, and wire vibration), self-turning adaptive control system.

Dr. ir. D. F. Dauw et al - Introduced some suitable detection techniques to improve accuracy and cutting position. Studied methodological awareness progress Wire EDM accuracy the system which is eagerly available on commercial wire EDM machines is based on the on-line tracking and control of the wire position. The variation of the wire position relative to the programmed wire path position is continuously measured and corrections are being made during the machine cutting. This technique allows cutting complex shapes, arc paths, and contours at a much faster cutting speed as compared to conventional wire EDM machines. Practical examples are discussed and the economic importance is asserted. Three conditions (rough cut with cutting speed $300mm^2$/min, cutting corner strategy on standard machines, and

optical sensor detection technique) are compared, where each time the cutting conditions are differing but the geometry of the contour is same. Wire displacement measuring principle is explained to measure wire position while machining. Wire vibration measurement and analysis devices were used for measuring wire vibrations during cutting, wire vibrations in a dielectric fluid, low-frequency wire vibration during cutting, wire vibration during machining.

N. Kinoshita et al.1984 Developed measuring method of wire vibration in the wire-EDM process to calculate approximately the width of the groove which depends in the lead of actions of electrode wire. Used wide range of machining conditions, mechanical behavior of wire is observed dynamically in the machining process. Described four experimental results and discussed those were, "shape of the wire when Discharge power is off, Effect of wire feed rate, Effect of feed direction, corner machining". N. Kinoshita et al.1987 developed and introduced a mathematical expression and new guide system of electrode wire to cut taper shapes using wire-EDM and also experimentally discussed angle errors while taper cutting. The boundary conditions and resolution of the second order ordinary differential equation can be found in Kinoshita et al. 1987

Mu-Tian Yan et al. has been developed a closed-loop wire tension control system to improve the accuracy of machining. To examine the dynamic performance of a closed-loop wire tension control system one-step-ahead adaptive controller and PI controller were engaged. Dynamic absorbers were added to idle rollers of wire transportation mechanism to reduce the vibration during feeding.

B. Ravani et al. developed a subdivision algorithm with kinematic analysis and normalization of the contour curves was used to achieve required actions of the machine tool axes. Build up numerical control (NC) of wire electric discharge machining from desired cut profile. Generating corners with small radii such as high curvatures, a geometric path lifting algorithm method is offered the machining gap and prevents gauging of wire breakage. Explained cut profiles for traveling using modeling, toolpath generation (kinematics of five-axis wire cut EDM system, machine tool motion), and incremental toolpath approximation.

J. A. SANCHEZ et al. discussed computer simulation software in taper cutting wire electrical discharge machining (WEDM) to predict the angular errors, based on the earlier research work but it considers friction into account between wire and guide during machining. The design of experiments (DoE) techniques is used to predict the angular errors in taper cut wire EDM machining process by changing the process parameters. Both Finite element model (FEM) simulation and Design of experiment (DoE) results have been validated through experimental tests in industrial conditions. ONA Prima E-250 WEDM machine has been used for machining process and dimensional measurements have been carried out on a Zeiss 850 Coordinate Measuring Machine. Conducted experiments with different Brass wires and different work materials 1.CuZn37 and AISI D2 tool steel, 2.Wire composition Base material: CuZn20 Coating: CuZn50 and AISI D2 tool steel, 3. Brass wire 0.25 mm 900 Nmm72 DIN 160 and Tool steel DIN X210CrW12.

S. Sarkar et al. 2011 Discussed wire lag and gap force to achieve high precision and accuracy. To understand the wire lag experience during cutting cylindrical job analytical model has been developed. Using known wire lag value is possible to modify the path to generate a high precision profile. An in-depth study on wire lag phenomenon has been carried out. Under any given condition of machining to predict wire lag and gap force intensity an analytical method has been introduced. An effective method has been proposed based upon developed analytical model to eliminate inexactness using wire lag compensation technique. (S. Sarkar et. al 2005) Explained single pass cutting operation using modeling and optimization of WEDM. Provided best control settings on a wire EDM machine to solve optimization. Developed, advanced artificial neural network to model the machining process. Considered cutting speed, surface roughness, and dimensional deviation have been considered as three most important parameters to measure process performance.

A.B. Puri et al. Almost all the control factors have been studied simultaneously to establish the trends of variation of a few important machining criteria with various control parameters. A rough cut followed by a trim cut has been considered as a machining operation. Those control factors for rough cut; pulse on time (T_{ON}), pulse off time (T_{OFF}), and pulse peak current (I_P) for rough cut, and ten control factors for trim cut followed by rough cut; pulse on time (T_{ON}), corresponding duty factor (D), pulse peak current (I_P), pulse peak voltage (V_P),

wire feed velocity (W_F), wire tension (W_T), servo-set spark voltage (*SV*), dielectric flow rate (*FR*), wire offset and cutting speed for trim cut. In a practical situation, it is a very difficult situation to select the best parametric combination, Taguchi L_{27} (3^{13}) orthogonal array has been used to reduce the experimental runs. The main influencing factors were determined, such as average cutting speed, surface finish characteristic and geometrical inaccuracy caused due to wire lag. Concluded so many points; (i) pulse on time, pulse off time and pulse peak current were affected mostly average cutting speed (V_C) during rough cutting; constant cutting speed and pulse on time during trim cutting. (ii) Pulse peak current mostly influenced surface roughness (Ra) during Rough cutting; pulse on time, pulse peak voltage, servo spark gap set voltage, dielectric flow rate, wire tool offset and constant cutting speed during trim cutting; concluded one more important i.e. Due to wire lag can't produce the highest productivity with the best surface finish at least in a single set of parametric combination.

Bijaya Bijeta Nayak et al.– explained utility theory concept. To determine the optimal process parameters in wire electrical discharge machining process during taper cutting operation, multi-response optimization approach has been studied. Taken part thickness, taper angle, pulse duration, discharge current, wire speed and wire tension as process parameters to do experiments and angular error surface roughness, and cutting speed as responses. Taguchi's L27 has been used to complete the experiment with less no. of experimental runs. Studied about utility theory has been implemented to overcome the limitation of traditional Taguchi method can't sufficient to solve a multi-response optimization problem.

Research objective

- To study the angular error during WEDM taper cutting process using FEM analysis as well as experimental analysis

- To study the contact stresses between the wire and guide using FEM analysis.

- To study the influence of process parameters during WEDM taper cutting process and obtain the best performance output using nature inspired optimization algorithms.

Chapter 3

Finite Element Analysis

3.1 Finite Element Analysis

The ultimate purpose of a finite element analysis is to recreate mathematically the behavior of an actual engineering system. In other words, the analysis must be an accurate mathematical model of a physical prototype. In the broadest sense, this model comprises all the nodes, elements, material properties, real constants, boundary conditions, and other features that are used to represent the physical system. In FEA large problem divides into smaller parts, called finite elements. Type of Meshing is an important role in FEM Analysis to achieve accurate results. No. of nodes and elements depends on the type of mesh, in the finer mesh nodes and elements are increases and preferable in precision matters.

3.2 Assumptions

Here, my aim is to find the deformation of the wire in taper cutting using Wire Electrical discharge machining (WEDM). Deformation has been achieved by creating tension on wire part using finite element analysis.

The following assumptions have been considered when developing the model:

- The effect of the forces acting on the wire due to the EDM regime is not included. The only external force is the axial force imposed by the machine itself.
- Only the upper-half of the wire has been modeled. It is assumed that the behavior in the lower half will be identical.
- Vertical displacement of the upper-end section of the wire is avoided.
- The lower-end of the upper-half of the wire is displaced horizontally to the ideal center point of the problem, i.e., the point at an equal horizontal distance from both guides.
- Plastic behavior of the wire is considered.

3.3 Type of wire and Guide

Ansys workbench R15.0 academic version software has been used to analyze the deformation and contact stresses when the wire in tension. Properties of wire and guide material play an important role to find the wire behavior at the needed position. Brass wire CuZn37 and Sapphire (Al_2O_3) as guide material was taken in the analysis.

3.3.1 Brass – copper-zinc alloy – CuZn37

Brass wire CuZn37 consists of 63% copper and 37% zinc. The product features very good mechanical properties (shown in table 3.1) and corrosion behavior comparable to copper. The good conductivity and the outstanding bending proof performance make it the favorite choice for heating applications. Furthermore, brass bare wires are suitable for electric discharge removal of material (spark erosion).

Some typical uses of CuZn37

Electrical use

Lamp caps, lamp holder and switch components.

Hardware use

General copper smithing work; chain; eyelets, fasteners, hinges, kicking plates, locks, fingerplates, and wire brushes.

Mechanical use

Miscellaneous cold presswork products, including instrument covers and containers, and blanked articles, such as instrument plates and wheels; cold-headed items including pins, rivets, and screws; springs; ink containers for ball-point pens; automobile radiator tanks; torch and flashlight cases; reflectors.

Table3-1 Mechanical properties of CuZn37 wire

S No	Property	Minimum value	Maximum Value
1	Density (kg/m^3)	8550	8550
2	Elongation (%)	10	57
3	Fatigue failure (MPa)	100	170
4	Tensile strength (MPa)	330	500
5	Yield Strength (MPa)	140	430
6	Young's modulus (MPa)	117000	117000

3.3.2 Sapphire Al_2O_3

Sapphire, also known as aluminum oxide is a single crystal form of corundum. It is in the purest form with no porosity or grain boundaries, making it theoretically dense. The combination of favorable chemical, electrical, mechanical, optical, surface, thermal, and

durability properties make sapphire a preferred material for the high-performance system and component designs. For various semiconductor applications, sapphire is the best choice in comparison with other synthetic single-crystals.

Table 3-2 Mechanical and thermal properties of Sapphire Al2O3

S No	Property	Value
1	Density, g/cm^3	3.98
2	Hardness (daN/mm^2)	1800 parallel to C-axis, 2200 perpendicular to C-axis, Mohs: 9
3	Young Modulus, Gpa	345
4	Poisson ratio	0.25-0.30
5	Tensile strength, MPa	400 at 25°, 275 at 500°, 345 at 1000°
6	Specific heat, J/(kg*K)	105 at 91°K, 761 at 291°K
7	Thermal coefficient of linear expansion, K^{-1},at 323K	6.66×10^{-6} parallel to optical axis, 5×10^{-6} perpendicular to optical axis
8	Thermal conductivity, W/(m*K) at 300K	23.1 parallel to optical axis, 25.2 perpendicular to optical axis

Key Properties

- Hard, Wear-resistant
- Excellent Dielectric properties from DC to GHz frequencies
- Resists strong acid and alkali attack at elevated temperatures
- Good thermal conductivity
- Excellent size and shape capability
- High strength and stiffness
- Available in purity ranges from 94%, an easily metallizable composition, to 99.8% for the most demanding high-temperature applications.

Applications

Sapphire materials and components have exceptional properties that are useful in many electronic, photonic or optical applications. End-uses include optical windows, laser

optics, lasing rods, lenses, micro-optics, reflectors, dummy wafers, silicon-on-sapphire (SOS) substrates, fixtures for high-temperature or high-pressure equipment, carrier plates or substrates for blue light-emitting diodes (LEDs) and laser diodes, high-speed integrated circuit (IC) chip substrates, microwave plasma tubes, flash lamp tubes, infrared (IR) detectors, and fiber optic lenses.

Because of their high hardness and wear characteristics, jewel bearings, bearing balls, valve balls, gage or styli points, wear parts and jewel pivots are often made from sapphire and ruby. Sapphire's optical transparency and wear resistance also makes it very useful for optical windows; point-of-sale (POS) scanner windows, liquid crystal display (LCD) projector windows, and watch faces.

3.4 Wire Tension

Depends on the axial force in the machine is set in the vertical position of the wire; its value must take friction into account. Thus, applying the well-known Eq. (1) for flexible wires the values of axial forces to be applied by the machine (i.e., in vertical position) can be obtained. These values are also included in figure 3.1 as a function of taper angle.

$$\frac{T_d}{Tu} = e^{\mu\theta} \quad \ldots\ldots\ldots\ldots\ldots\ldots\ldots\ldots\ldots\ldots (1)$$

Where, T_d = axial force acting on the wire at the exit of the guide

T_u = axial force acting on the wire applied by the machine

μ = coefficient of friction

θ = contact angle between wire and guide

Table3-3 T_d values at different T_u and angles

Tension(T_u) In newton	Angle(^{0})	Tension(T_d) in newton
14	10	13.29
	20	12.61
16	10	15.18
	20	14.41

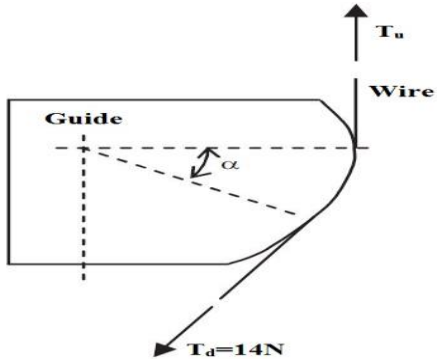

Figure 3-1 Axial forces acting on the wire at the entrance of the guide and at the exist of the guide

3.5 Simulation of the Finite Element Model

Open static structural

Workbench > Toolbox > Static Structural

Define Material Properties

Workbench > Static structural > Engineering Data > Brass > Toolbox > Sapphire > toolbox

Modeling

Workbench > Static Structural > Geometry > Design Modeler

Analysis Procedure

I. Import model : Workbench > Static Structural > Model > Outline > Geometry > Brass > Geometry > Sapphire

II. Connections : Mechanical > Outline > connections > contacts > Scope > Contact(=Brass) > Target (=Sapphire) > Definition > Type(Frictional) > Friction Coefficient (= 0.3) > Geometric modifications > Interface Treatment(=Adjust to Touch)

III. Meshing : i. Outline > Mesh > Sizing > Relevance enter(Fine) > Smoothing (High) > Transition (Fast)

ii. Outline > Mesh > Refinement > Definition > Refinement (= 1) Shown in figure 3.2

IV. Applying Boundary Conditions:

i. Load: Outline > Static Structural > Loads > Force > Details > Scope > Geometry > Apply (=Top face of the Brass Wire) > Definition > Magnitude (= Value) Shown in figure 3.3

ii Load: Outline > Static Structural > Loads > Force2 > Details > Scope > Geometry > Apply (=Bottom face of the Brass Wire) > Definition > Magnitude (= Value)

iii. Fixed Support: Outline > static structural > supports > Fixed Support>Details>Scope> Geometry (=Sapphire)

V. Getting Solutions

Outline > Solution > Deformation > Directional > Details > Geometry (= Brass)

3.6 Elements

SOLID187 Element

The solid187 element is a higher-order 3-D, 10-node element. The element is defined by 10 nodes having three degrees of freedom at each node: translations in the nodal x, y, and z directions (shown in figure 3.4). SOLID187 has a quadratic displacement behavior and is well suited to modeling irregular meshes. It also has mixed formulation capability for simulating deformations of nearly incompressible elastoplastic materials and fully incompressible hyperelastic materials.

Nodes 10

I, J, K, L, M, N, O, P, Q, R

Degrees of Freedom 03

UX, UY, UZ

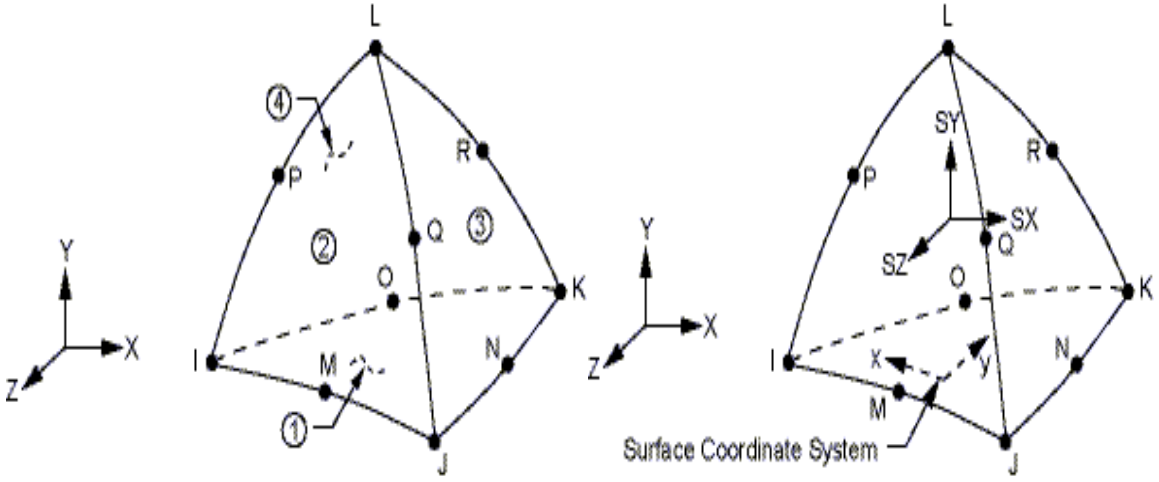

Figure 3-2 Geometry of the SOLID187 and surface stress output representation

Special Features of SOLID187

The element has Plasticity Hyperelasticity, viscoelasticity, viscoplasticity/creep, elasticity, Stress stiffening, large deflection, large strain, nonlinear stabilization, and automatic selection of element technology, birth, and death, linear perturbation

SOLID186 Element Description

SOLID186 Homogenous Structural Solid is well suited to modeling irregular meshes. The geometry, node locations, and the element coordinate system for this element are shown

in figure 3.4. SOLID186 is a higher-order 3-D 20-node solid element that exhibits quadratic displacement behavior. The element is defined by 20 nodes having three degrees of freedom per node: translations in the nodal x, y, and z directions.

Nodes 20

I, J, K, L, M, N, O, P, Q, R, S, T, U, V, W, X, Y, Z, A, B

Degrees of Freedom 03

UX, UY, UZ

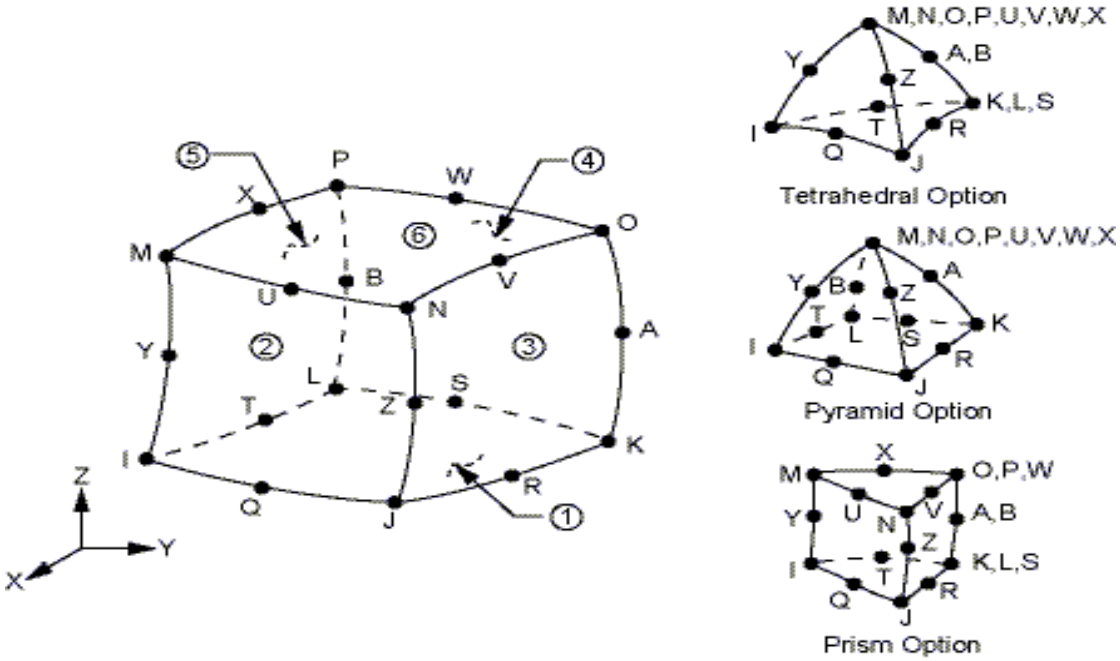

Figure 3-3 Geometry of SOLID186 Homogenous Structural Solid

This element also like SOLID186 supports plasticity, hyperelasticity, creep, stress stiffening, large deflection, large strain capabilities and etc. It also has mixed formulation capability for simulating deformations of nearly incompressible elastoplastic materials and fully incompressible hyperelastic materials.

Friction arises when two surfaces (or bodies) are in contact and in motion. Here also Sapphire and brass wire are in contact. The coefficient of friction describes the ratio of the friction force between two surfaces and the force pressing them together. μ is the coefficient of friction, which is an empirical property of the contacting materials. Coefficient of friction μ

= 0.3. For general Surface to surface contact, CONTAC171 and CONTAC174 are recommended

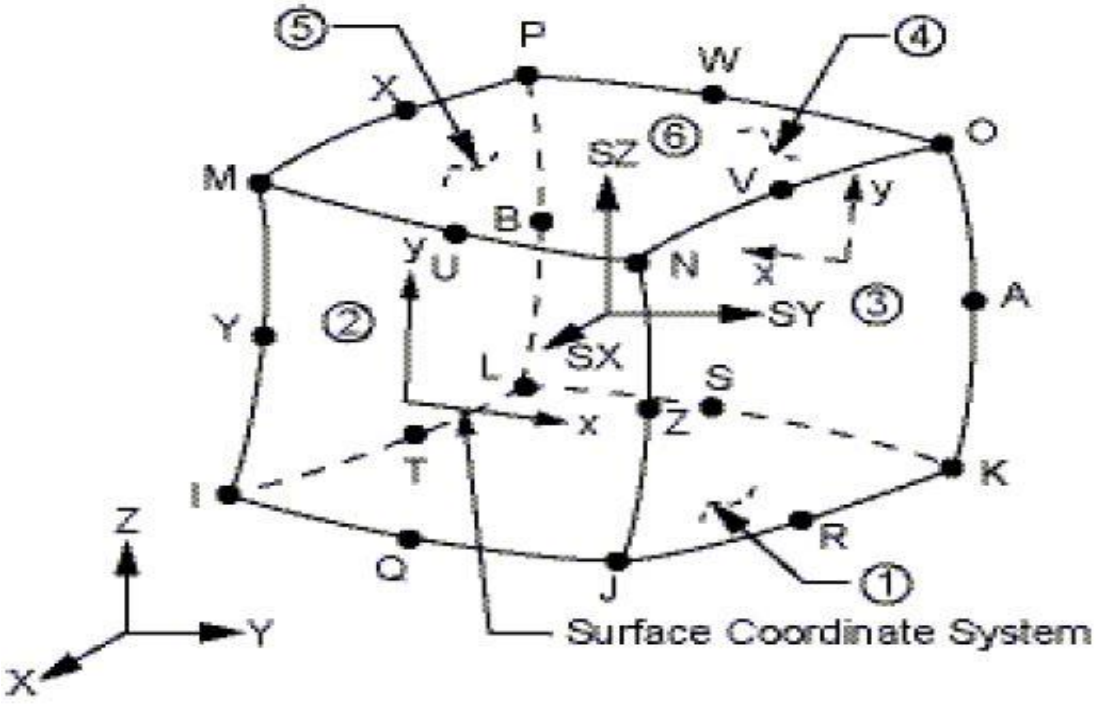

Figure 3-4 SOLID186 element stress output directions

.

CONTA174: This element is a 3-D, 8-node, higher-order quadrilateral element that can be located on the surfaces of 3-D solid or shell elements with midsize nodes. It can degenerate to 3 - 7 node quadrilateral/triangular shapes. ANSYS will automatically detect whether the underlying element is a super element.

Using Surface-to-Surface Contact Elements

ANSYS supports both rigid-to-flexible and flexible-to-flexible surface-to-surface contact elements. In problems involving contact between two boundaries, one of the boundaries is conventionally established as the “target surface”, and the other as the “contact surface”. For rigid-flexible contact, the target surface is always the rigid surface, and the contact surface is the deformable surface. For flexible-to-flexible contact, both contact and target surfaces are associated with the deformable bodies. These two surfaces together comprise the “contact pair”.

• The target surface is modeled with either TARGE170 for 3-D

• The contact surface is modeled with elements CONTA174.

Combination to define the complex target surface geometry in 3-D cases, the shape of the target surfaces is described by a sequence of triangles, quadrilaterals, straight lines, parabolas, cylinders, cones, and spheres, which can be represented with TARGE170. You can use any reasonable combination of low/high-order triangles and quadrilaterals to model a target surface with a complex, arbitrary geometry.

Element Surf154

Surface effect elements SURF154 (CREDITS **Collaborative Solutions Inc.)** surface effect elements are extremely useful tools in both structural and thermal analyses. These elements provide the user with more flexibility in applying loads to their model. SURF154 elements are used for meshing cylindrical area.

Surface effect elements have no physical properties. These elements are mainly used for loading purposes only. They are overlaid like a "skin" on structural element face. Structural surface effect element, SURF154; allow the user to define pressures in various manners:

• Application of a tangent pressure such as traction or an overall moment

• Pressure on a projected area such as a bolt load

The SURF154 element can be used with any lower- and higher-order structural element, with the exception of axisymmetric-harmonic elements

Modified Element

COMBIN14

Stiffness and damping coefficients can be a function of frequency. Used for modeling frequency dependent material.

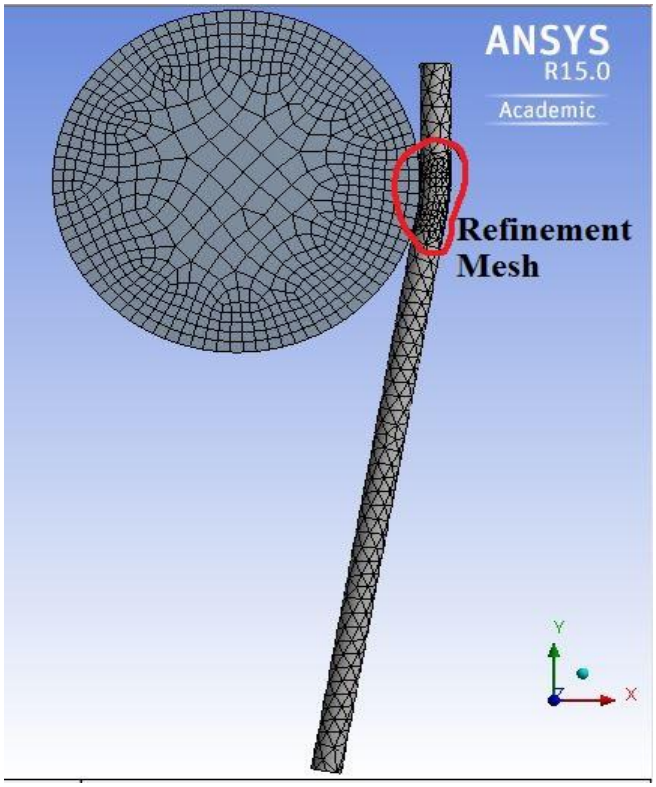

Figure 3-5 Refinement mesh is used at the contact point between the wire and the guide

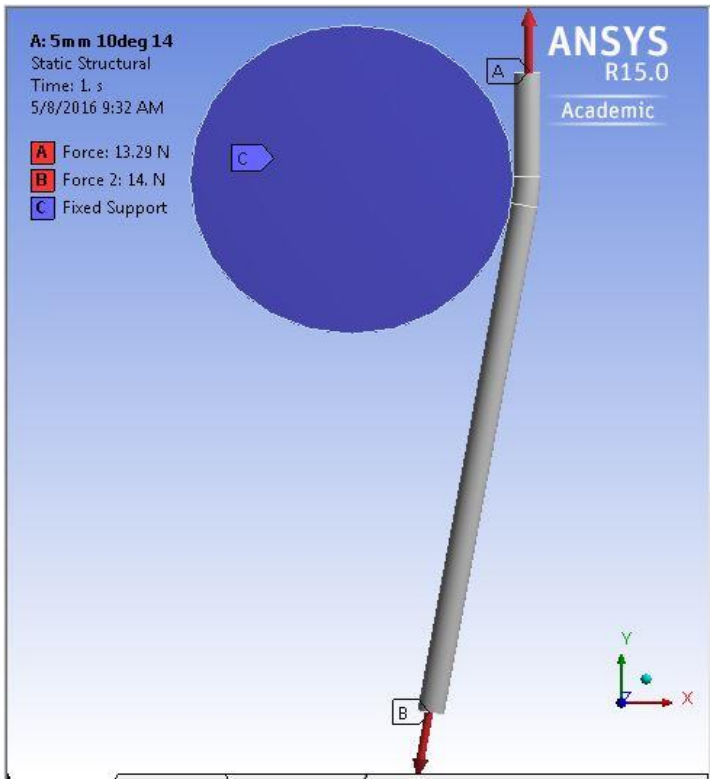

Figure 3-6 Applying boundary conditions on the wire and the guide

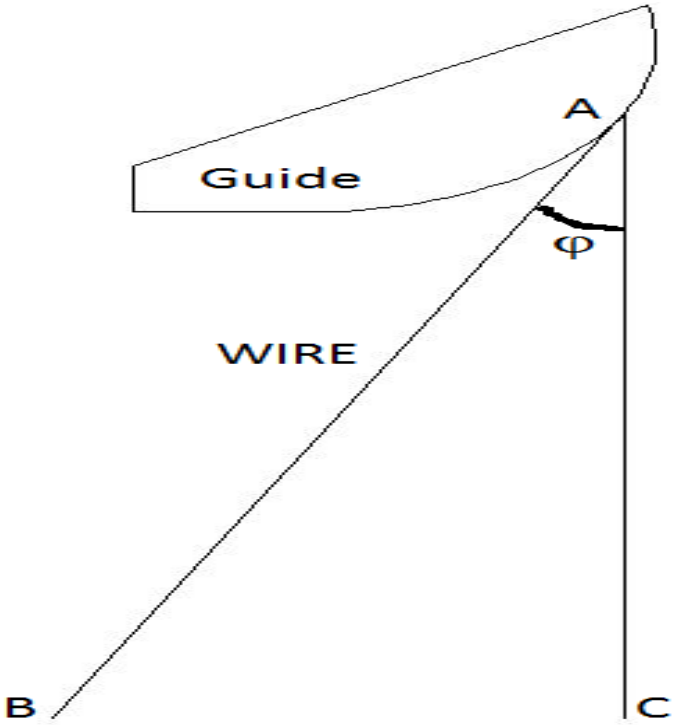

Figure 3-7 Geometrical representation of wire

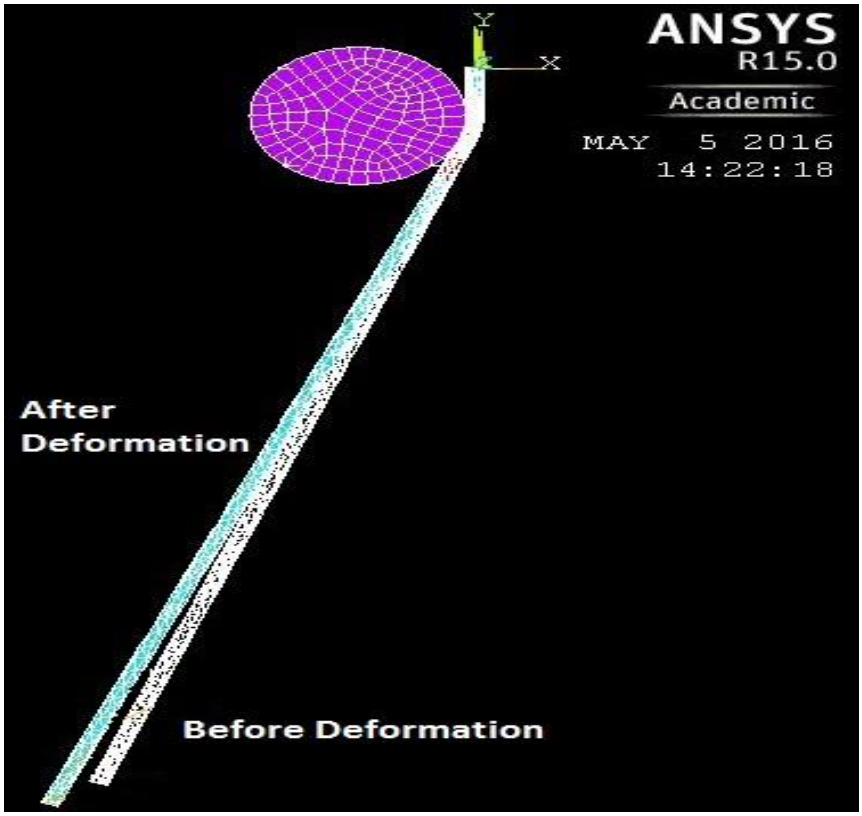

Figure 3-8 wire Deformation before and after

3.7 Angular Error

From figure 3.7 wire AB is in an inclined position with a guide and at the same time AB making φ inclination with line AC. Due to tension in the wire, the position of the wire moves towards or away from the line AC as shown in fig 3.8.That result is called Directional Deformation. Angular error has been calculated by using directional deformation

Length of the wire = 5 mm

Inclination of the wire = 10^0

Tension applied to the wire = 14N

Directional deformation of the wire = 0.034576

Angular error = 10.4026^0 or 10^0 24’ 09”

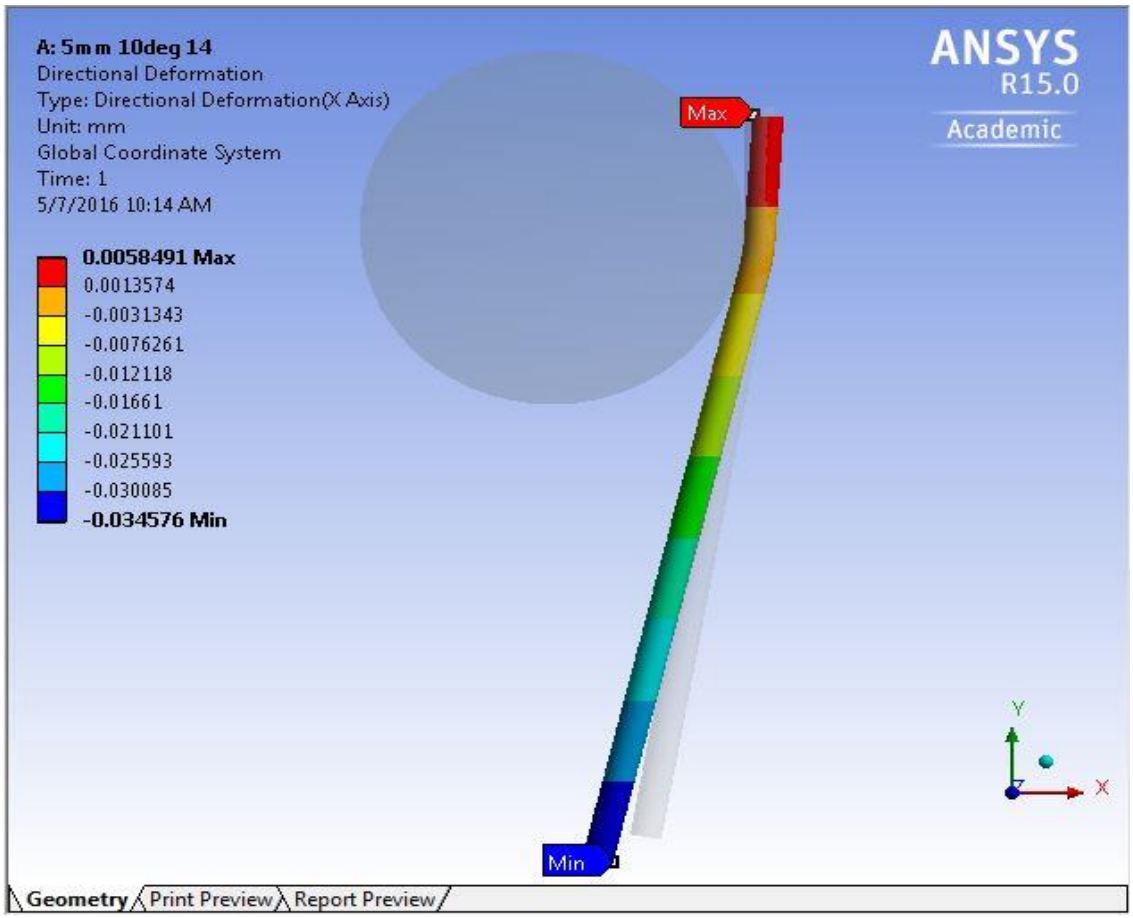

Figure 3-9 Deformation of 5mm wire at angle 10^0 and tension 14N

Length of the wire = 5 mm

Inclination of the wire = 10^0

Tension applied on the wire = 16N

Directional deformation of the wire = 0.01071

Angular error = 10.1242^0 or 10^0 07’ 27”

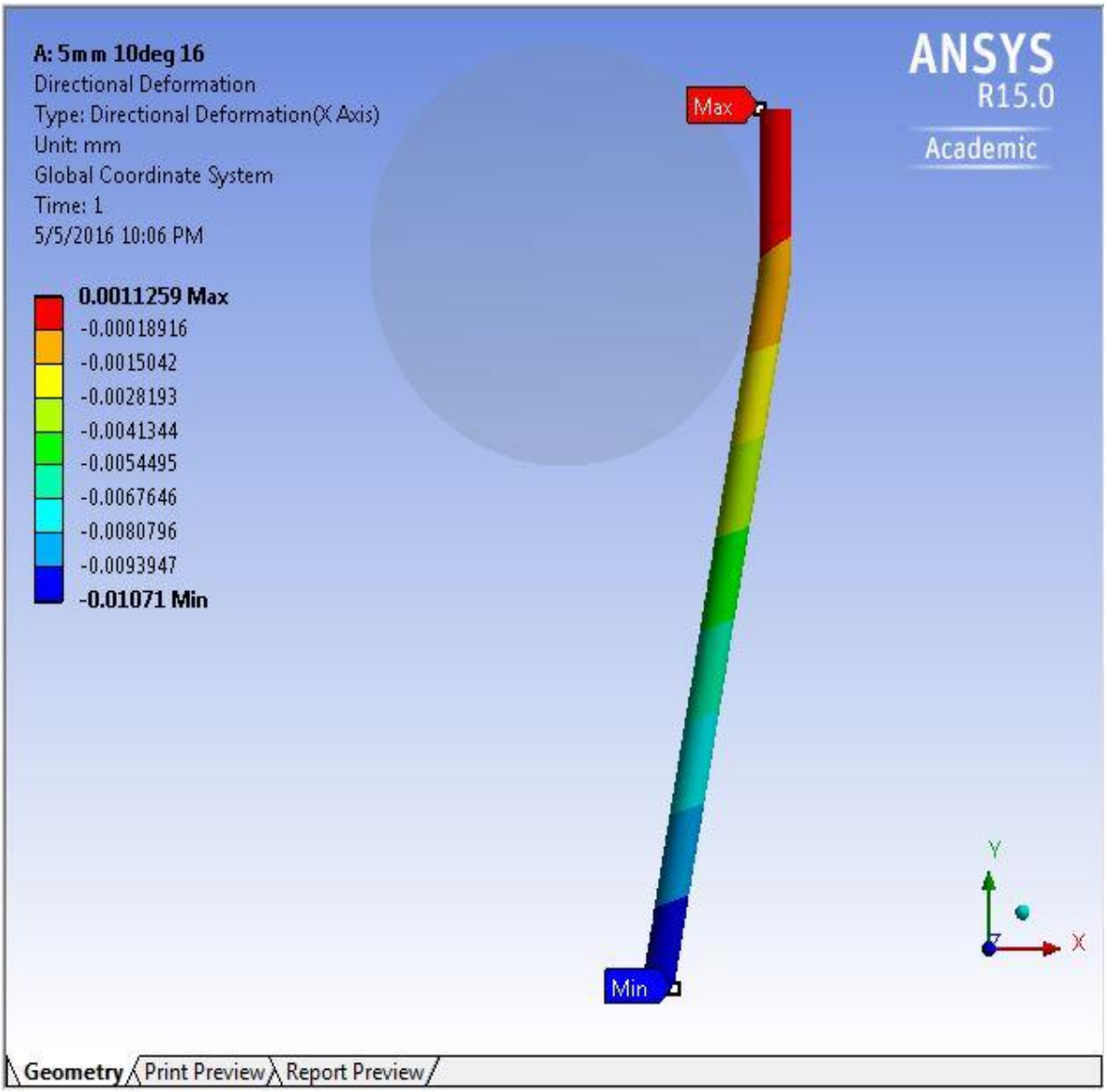

Figure 3-10 Deformation of 5mm wire at angle 10^0 and tension 16N

Length of the wire = 5 mm

Inclination of the wire = 20^0

Tension applied on the wire = 14N

Directional deformation of the wire = 0.018437

Angular error = 20.2249^0 or 20^0 13’ 29”

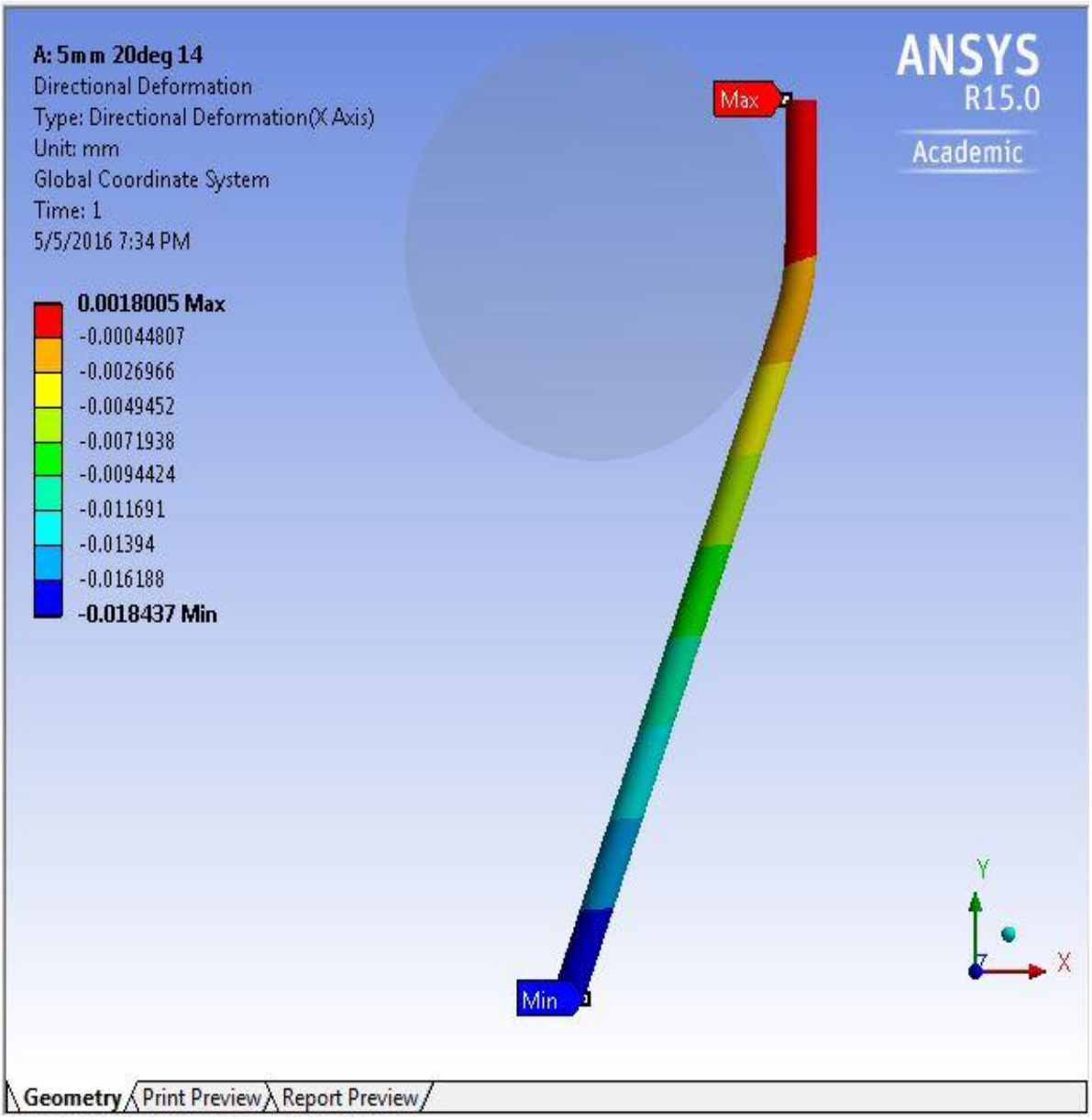

Figure 3-11 Deformation of 5mm wire at angle 20^0 and tension 14N

Length of the wire = 5 mm

Inclination of the wire = 20^0

Tension applied on the wire = 16N

Directional deformation of the wire = 0.013197

Angular error = 20.161^0 or 20^0 09’ 39”

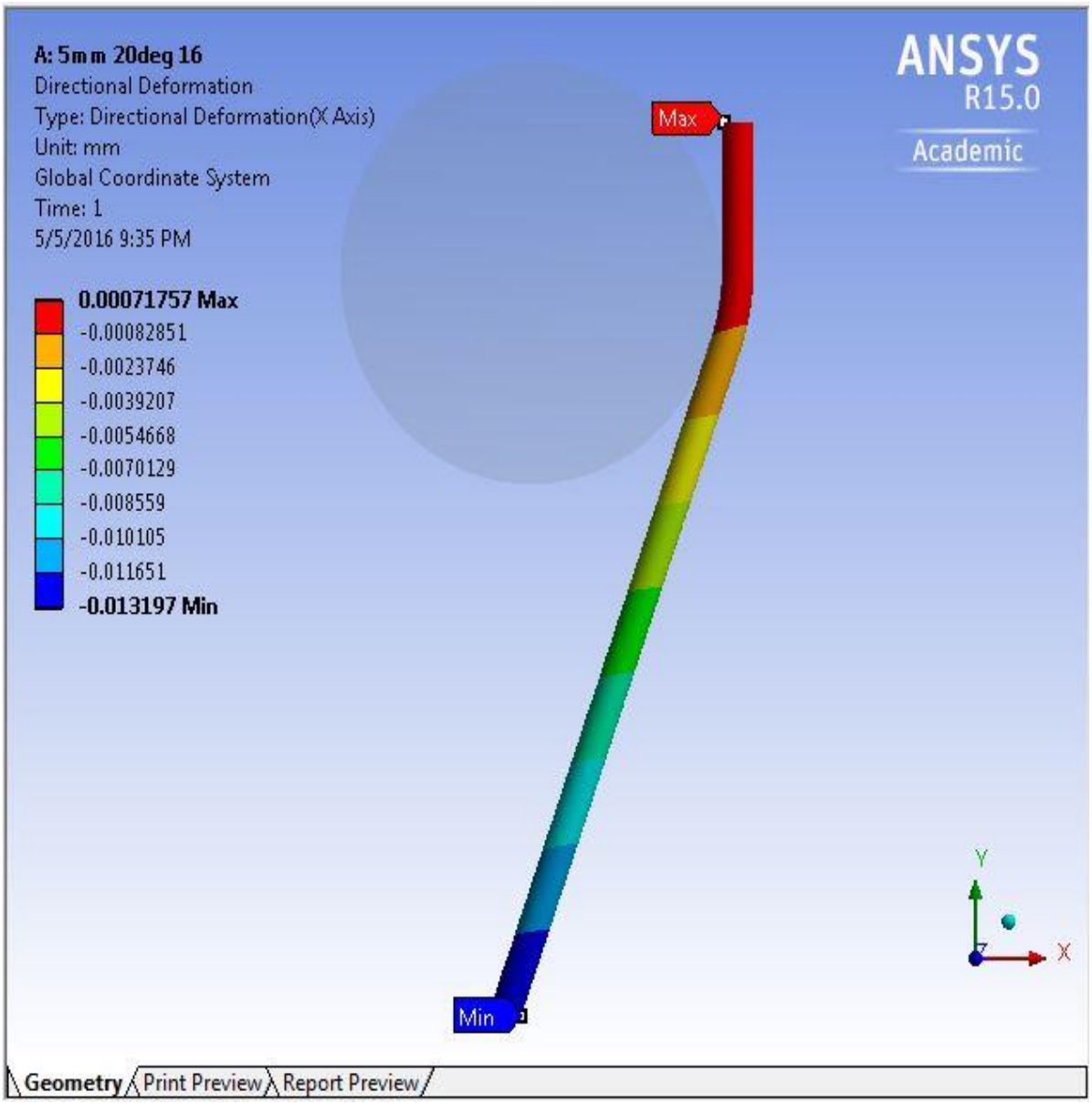

Figure 3-12 Deformation of 5mm wire at angle 20^0 and tension 16N

Length of the wire = 10 mm

Inclination of the wire = 10^0

Tension applied on the wire = 14N

Directional deformation of the wire = 0.045821

Angular error = 10.2667^0 or 10^0 16’ 00”

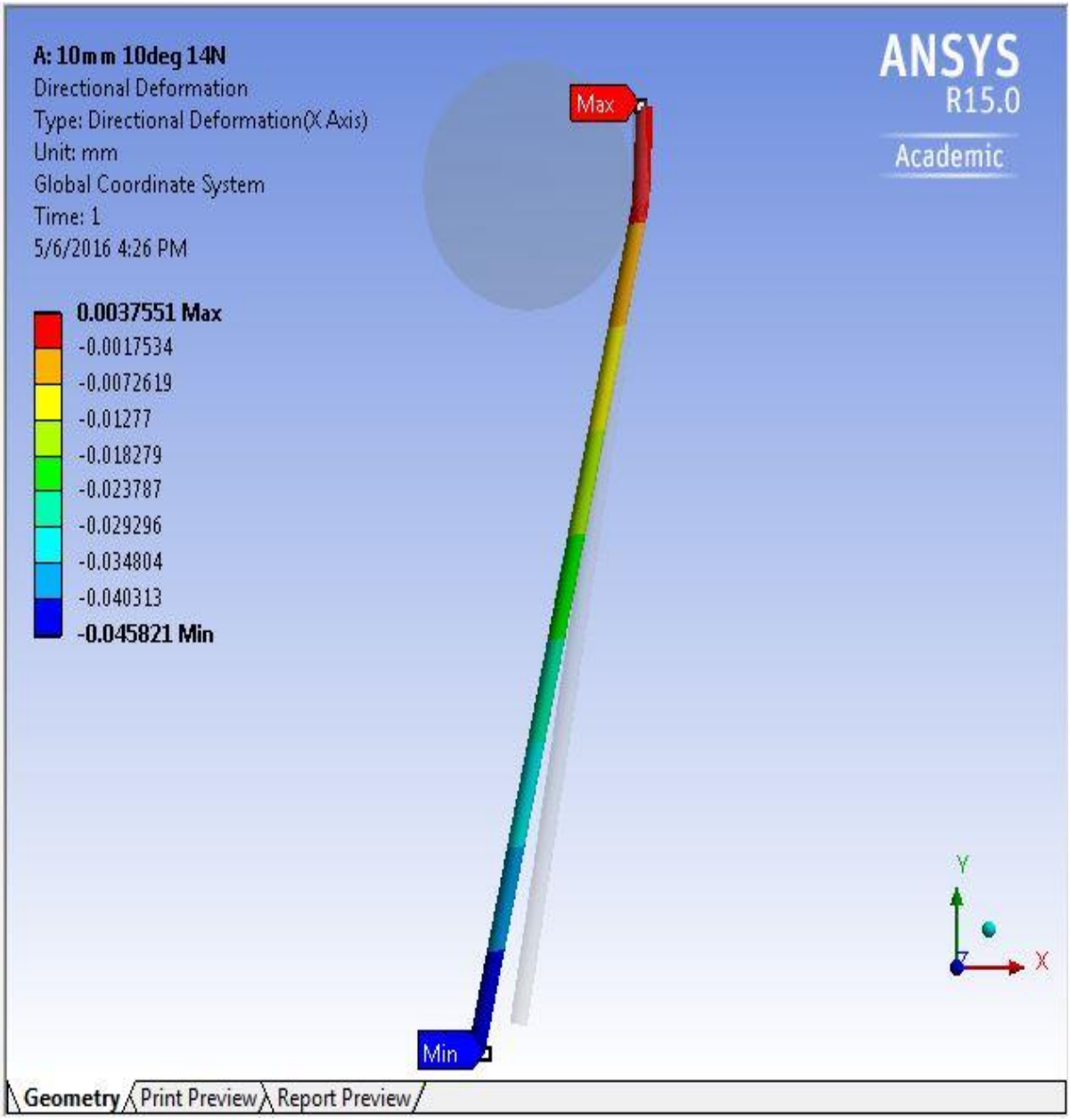

Figure 3-13 Deformation of 10mm wire at angle 10^0 and tension 14N

Length of the wire = 10 mm

Inclination of the wire = 10^0

Tension applied on the wire = 16N

Directional deformation of the wire = 0.053787

Angular error = 10.3133^0 or 10^0 18’ 47”

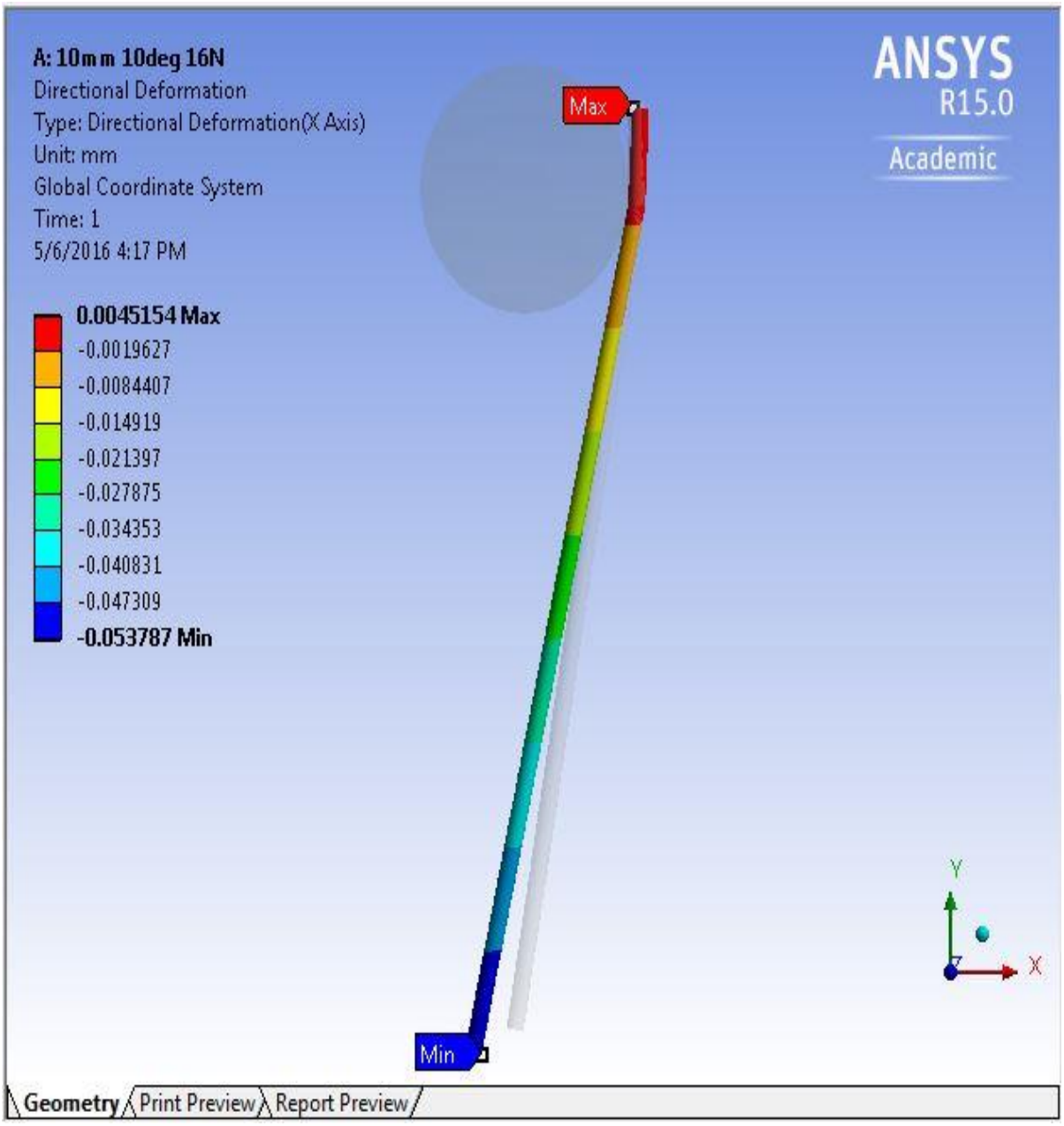

Figure 3-14 Deformation of 10mm wire at angle 10^0 and tension 16N

Length of the wire = 10 mm

Inclination of the wire = 20^0

Tension applied on the wire = 14N

Directional deformation of the wire = 0.028327

Angular error = 20.1512^0 or 20^0 09’ 04”

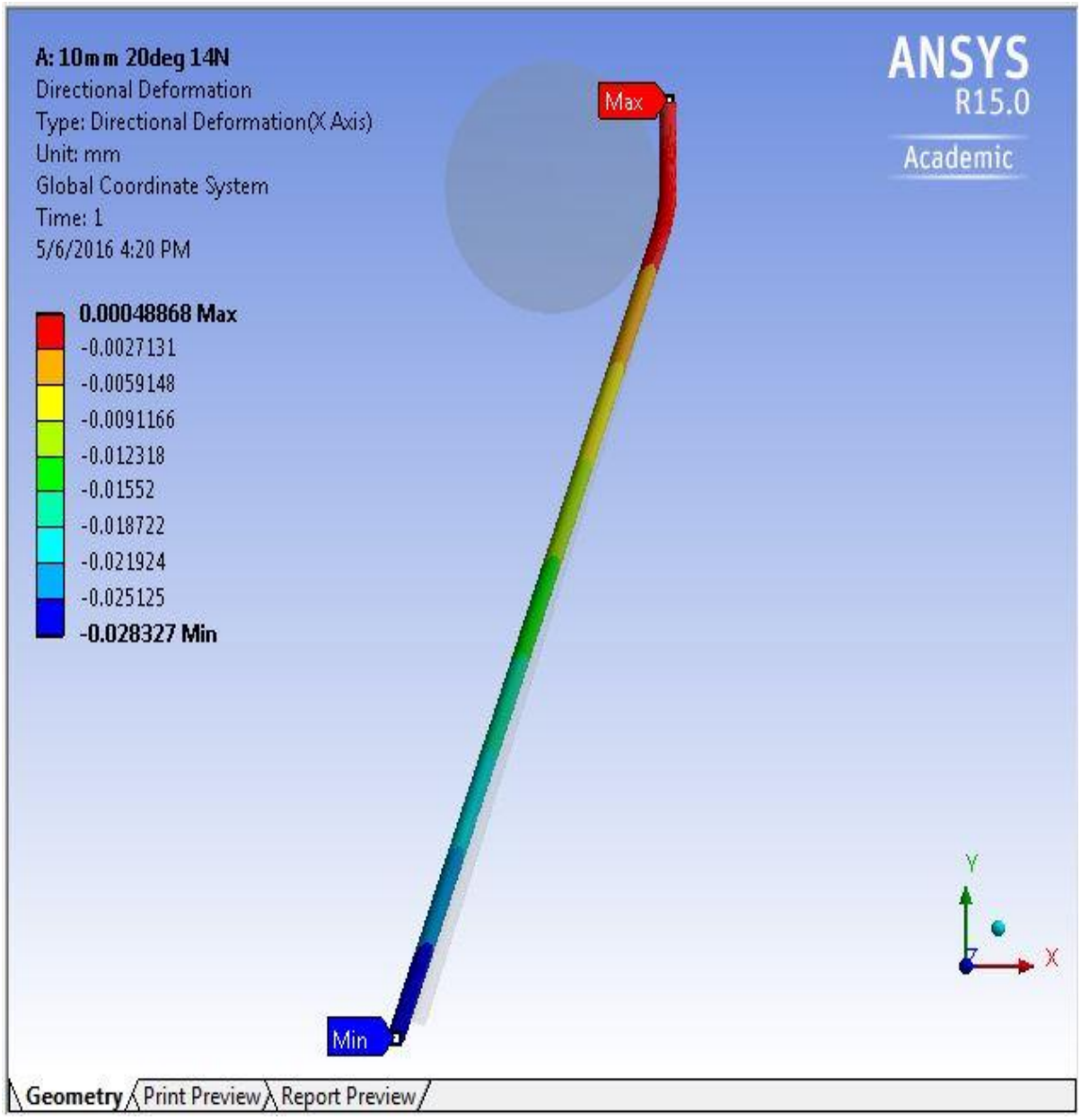

Figure 3-15 Deformation of 10mm wire at angle 20^0 and tension 14N

Length of the wire = 10 mm

Inclination of the wire = 20^0

Tension applied on the wire = 16N

Directional deformation of the wire = 0.040464

Angular error = 20.2471^0 or 20^0 14’ 49”

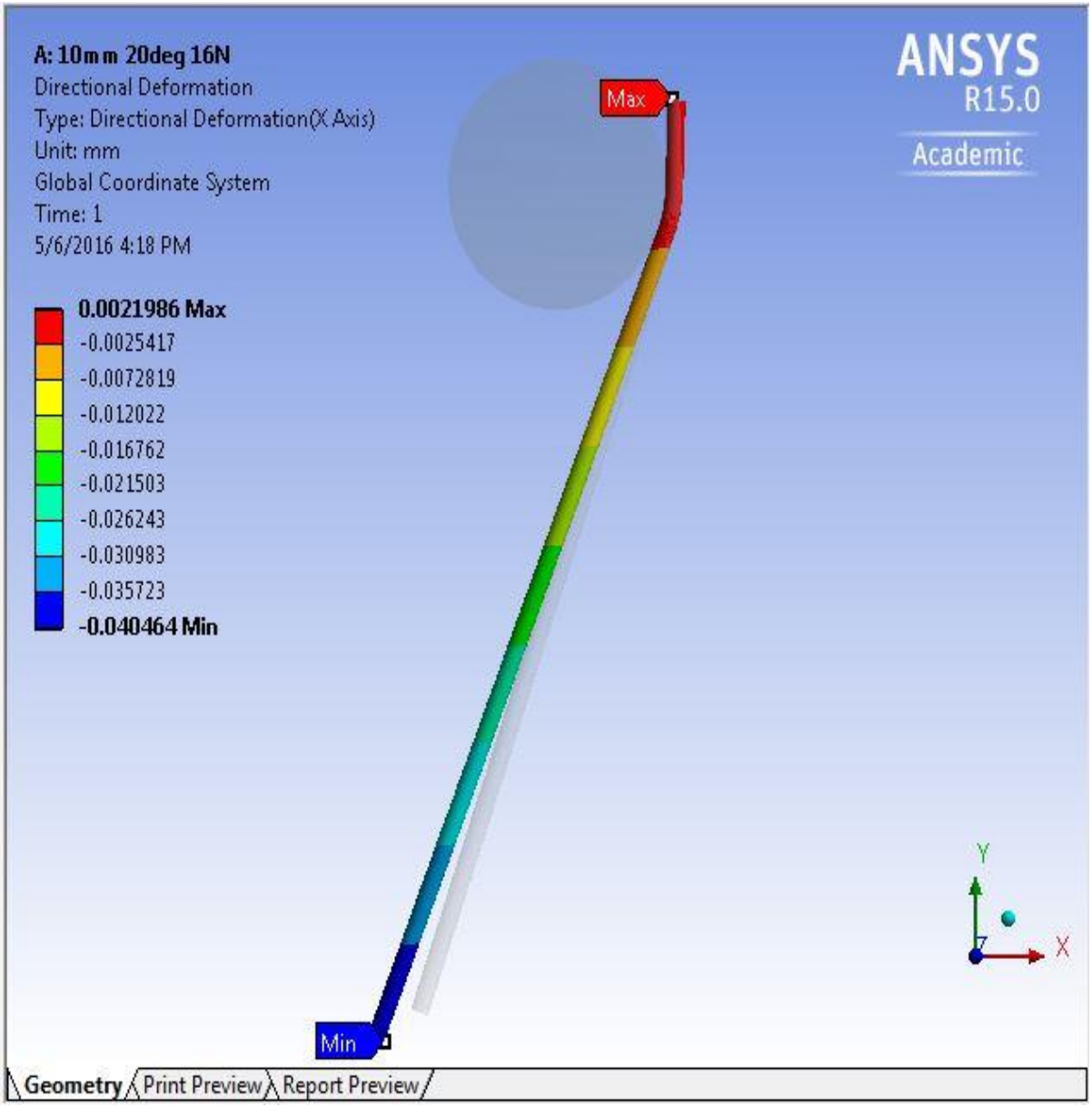

Figure 3-16 Deformation of 10mm wire at angle 20^0 and tension 16N

Length of the wire = 15 mm

Inclination of the wire = 10^0

Tension applied to the wire = 14N

Directional deformation of the wire 0.06345

Angular error = 10.2463^0 or 10^0 14’ 46”

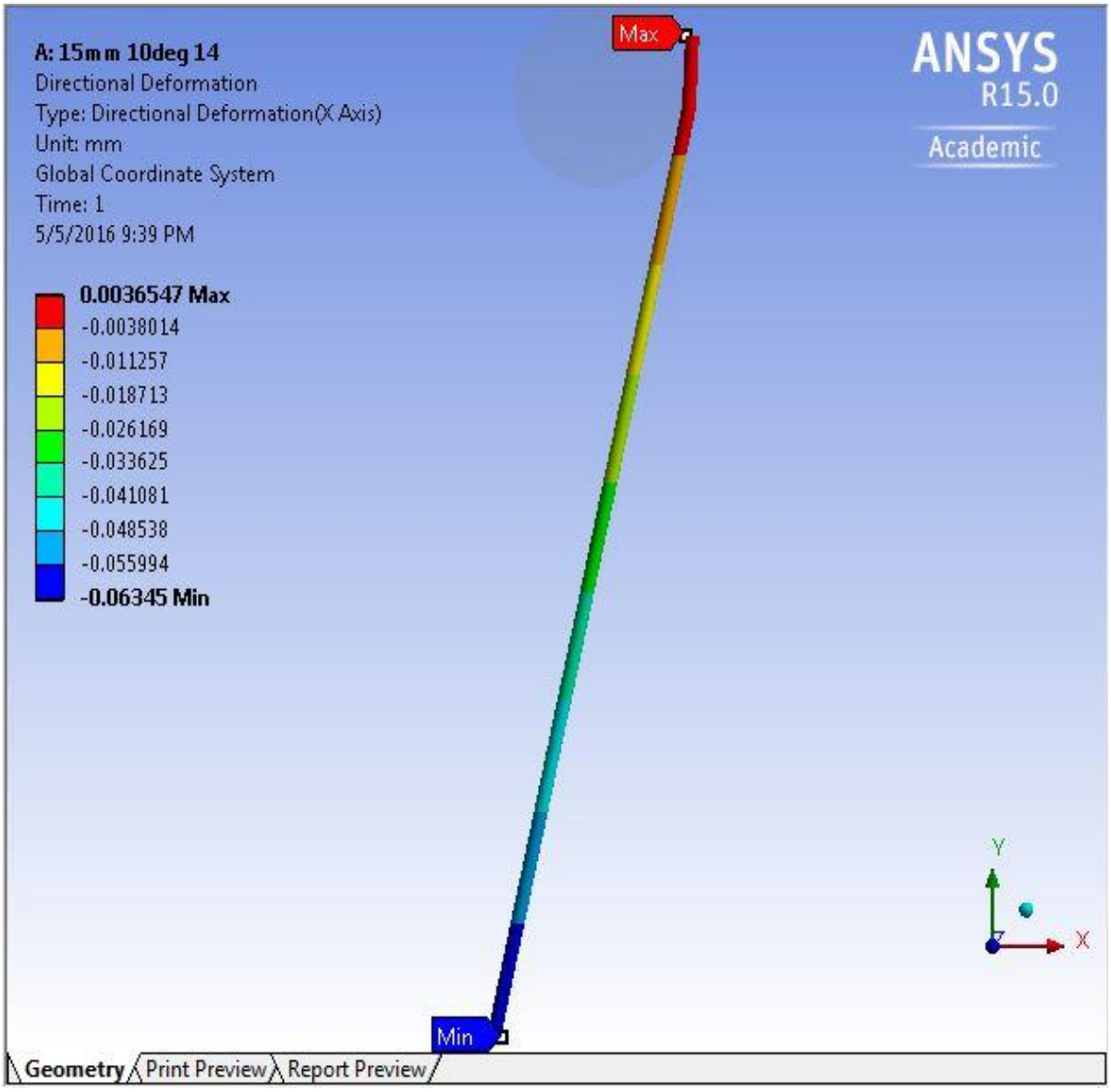

Figure 3-17 Deformation of 15mm wire at angle 10^0 and tension 14N

Length of the wire = 15 mm

Inclination of the wire = 10^0

Tension applied on the wire = 16N

Directional deformation of the wire = 0.063218

Angular error = 10.2453^0 or 10^0 14’ 43”

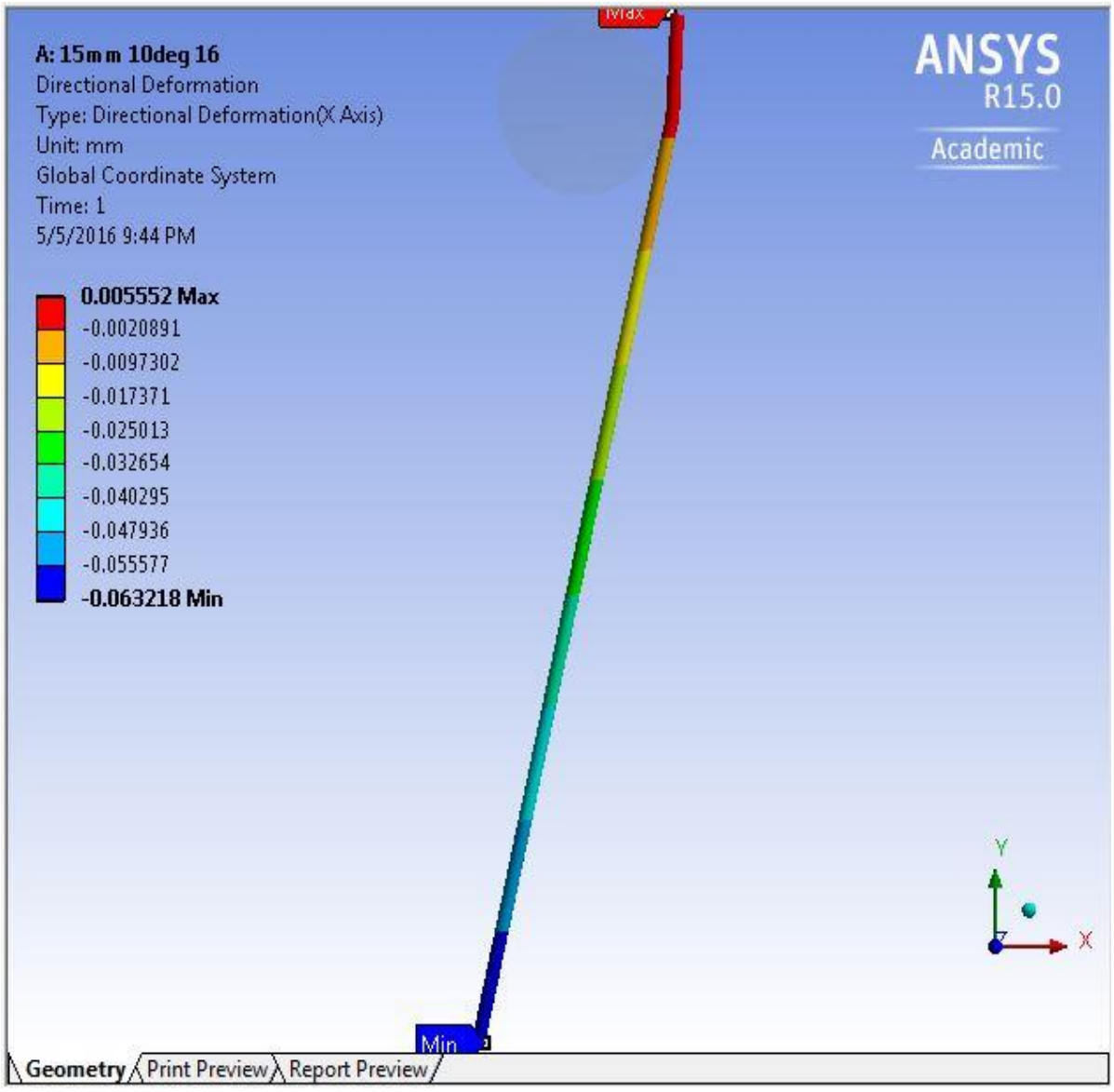

Figure 3-18 Deformation of 15mm wire at angle 10^0 and tension 16N

Length of the wire = 15 mm

Inclination of the wire = 20^0

Tension applied on the wire = 14N

Directional deformation of the wire = 0.032101

Angular error = 20.1305^0 or 20^0 07’ 49”

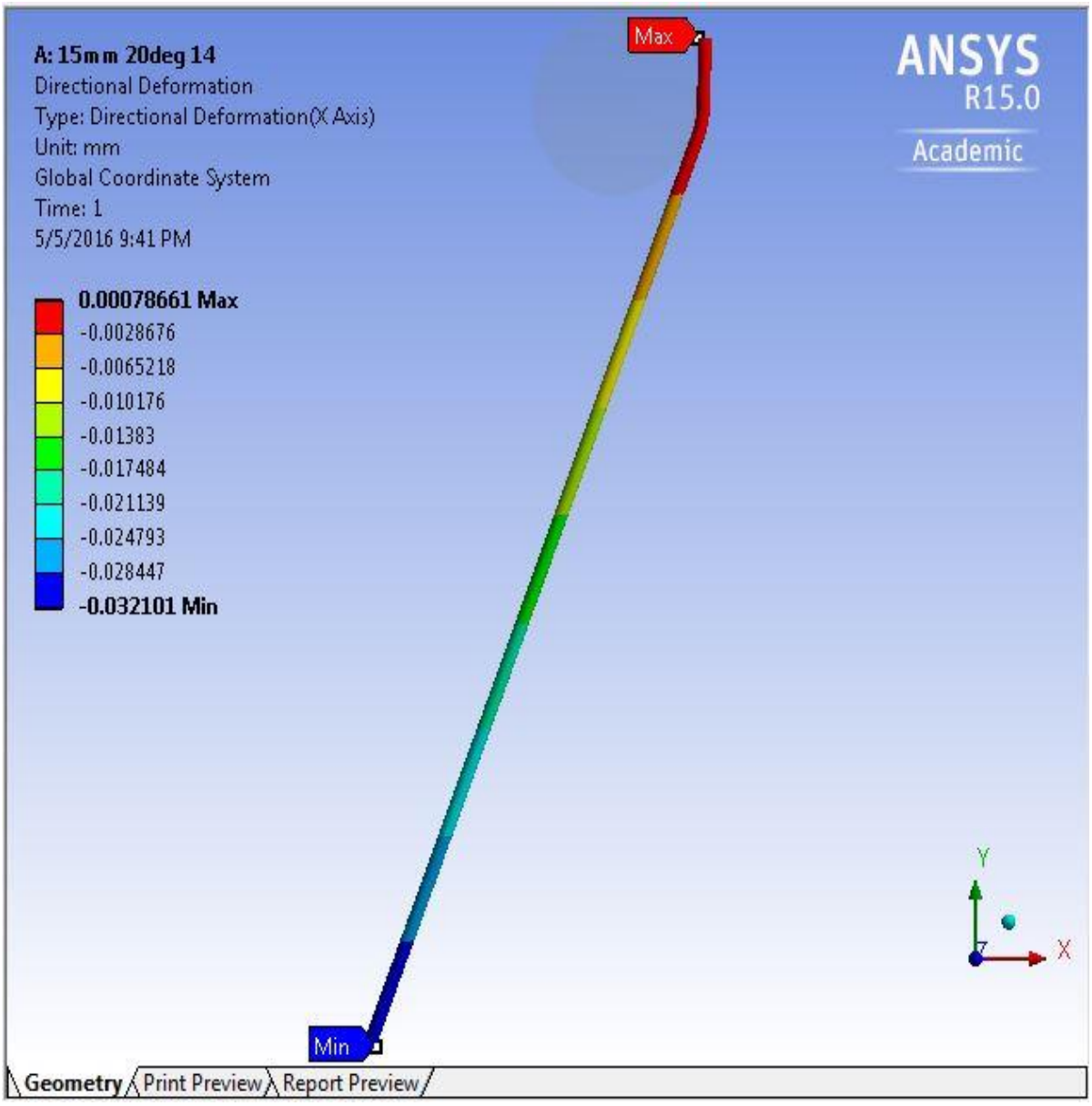

Figure 3-19 Deformation of 15mm wire at angle 20^0 and tension 14N

Length of the wire = 15 mm

Inclination of the wire = 20^0

Tension applied to the wire = 16N

Directional deformation of the wire = 0.047281

Angular error = 20.1923^0 or 20^0 11’ 32”

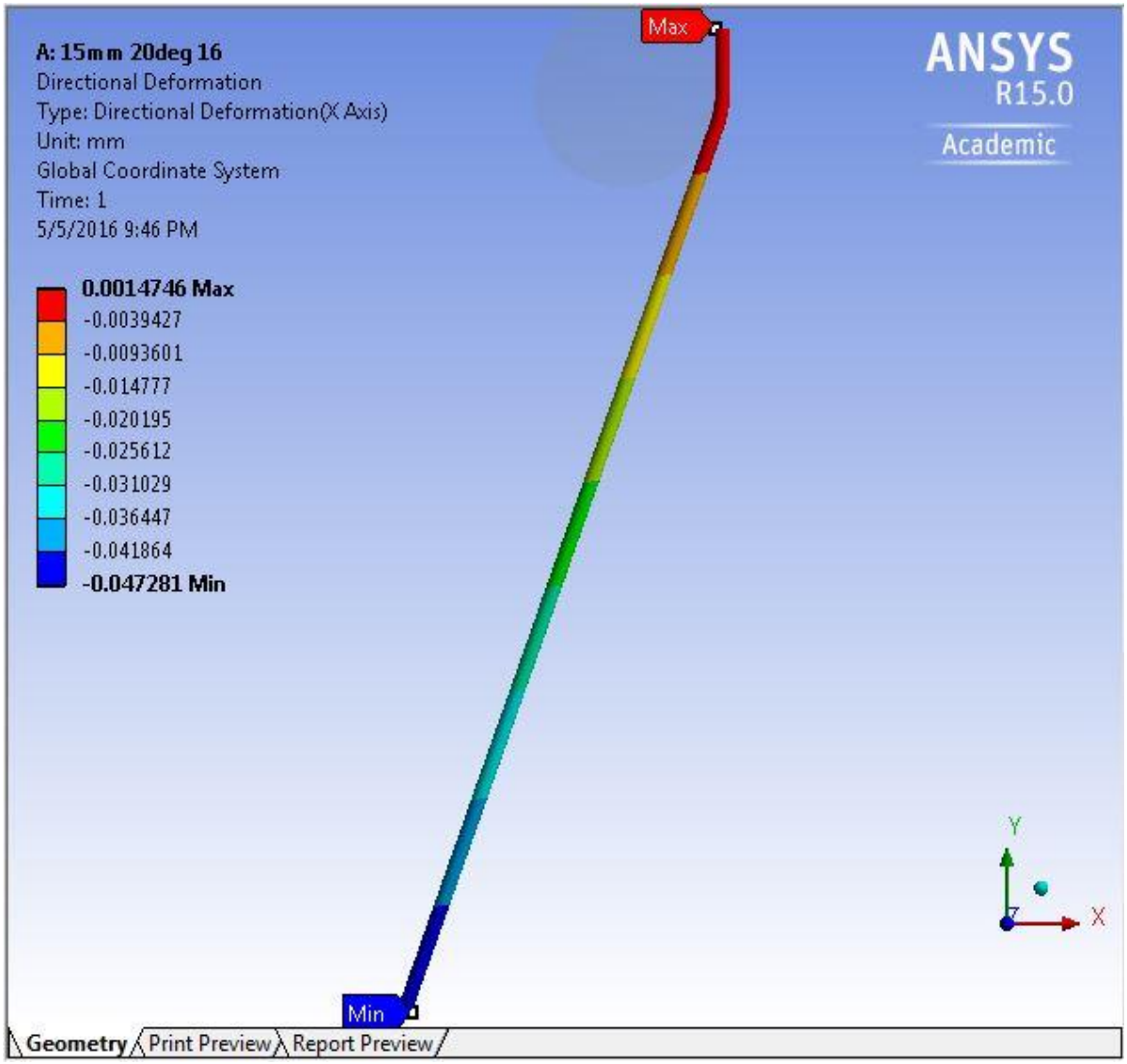

Figure 3-20 Deformation of 15mm wire at angle 20^0 and tension 16N

Chapter 4

Experimental Procedure

4.1 Experimental Details

The experiments were conducted on AC Progress V2 high precision CNC WEDM manufactured by Agie-Charmilles Technologies Corporation as shown in Figure 4.1 on this machine, all the axes are servo controlled and can be programmed to follow a CNC code which is fed through the control panel and has the following specification

Simultaneous control axis : X, Y, U, V, Z

Axis Travels : 350×250×256 mm

Maximum workpiece dimension: 750×550×256 mm

Maximum workpiece weight : 450 kg

U& V axis travels : ±70 mm

Maximum taper angle <˚/ Height : ±30˚/100mm

Figure 4-1 AC Progress V2 CNC-Wire Cut EDM Machine

4.2 Workpiece and Wire Electrode Material

The current study used AISI 316 stainless steel of diameter 75mm and thickness of 10mm, and 30mm respectively as the workpiece material. Soft wire electrode material CuZn37 of diameter 0.25 was considered due to high elongation and low yield strength.

4.2.1 AISI 316 Austenitic Stainless Steel

316 Austenitic stainless steel contains an addition of molybdenum that gives it improved corrosion resistance. This is particularly apparent for pitting and crevice corrosion in chloride environments. The austenitic structure of 316stainless steel gives excellent toughness, even at cryogenic temperatures. The chemical composition of the wire material is C = 0.08 max., Mn=2, Si=0.75, P=.045, S=.03, Cr=16-18, Ni=10-14, and N=0.1 and **Table** Show the physical and mechanical properties of the workpiece materials.

Table 4-1 physical properties of AISI 316

Physical Property	**Value**
Density	8.00 g/cm3
Melting Point	1375-1400°C
Modulus of Elasticity	193 Gpa
Electrical Resistivity	0.074x10-6 Ω.m
Thermal Conductivity	16.3 W/m.K at 100°C
Thermal Expansion	15.9x10-6 /K at 100°C

Table4-2 Mechanical properties of AISI 316

Mechanical Property	**316**
Tensile strength (MPa)	515
Compression Strength (MPa)	170
Proof Stress 0.2% (MPa)	205
Elongation A5 (%)	40

4.3 Important Process Parameters of WEDM Tapering Process

The proper selection of the machining parameters is desirable prior to staring of any machining process. WEDM tapering process is affected by various process parameters from those six important process parameters part thickness, taper angle, pulse duration, discharge current, wire speed, and wire tensions are considered in this experiment.

Part thickness: Part thickness refers to the thickness of the work piece which is considered as one of the important parameters in WEDM taper cutting process.

Taper angle: Taper angle or wire inclination angle is another important factor for taper cutting in WEDM. The maximum angle that can be obtained is a function of the work piece thickness and the mechanical behavior of wire.

Pulse duration: It is the sum of ignition delay time and discharge duration. Pulse duration which is represented in μs.

Discharge current: It is the most important machining parameter as it directly governs the spark energy. The maximum amount of amperage that can be used is governed by the surface area of the cut for a work piece-tool combination. A Higher value of discharge current results in higher material removal but in turn produces numerous adverse effects on the machined surface. It is measured in terms of Ampere.

Wire speed: Wire speed is also the important process parameter indicating the speed of the wire in WEDM. Higher wire speed results in less wire breakage, better machining stability, and slightly more cutting speed. It is represented in mm/s.

Wire tension: Wire tension determines how much the wire is to be stretched between upper and lower wire guides. More the thickness of job more tension is required. Within the considerable range, an increase in wire tension significantly increases the cutting speed and accuracy. However, improper setting of tension may result in the job inaccuracies as well as wire breakage. Wire tension is expressed in Newton.

Distilled water is used as dielectric in this experimental analysis. The table shows properties of distilled water.

Table 4-3 Distilled water properties

Distilled water property	Temp. (^{0}c)	Density (x1000 Kg/m^3)	Viscosity (Pa-s)	Kinematic Viscosity (m^2/s)	Surface Tension (N/M)	Bulk Modulus (GPa)	Thermal Expansion coefficient(/^{0}c)
Value	100	0.958	$2.82x10^{-4}$	$2.94x10^{-7}$	$5.89x10^{-2}$	2.07	$7.50x10^{-4}$

4.4 Input Parameters and Output Responses

Taguchi L_{16} orthogonal array is used in this experimental analysis to reduce the number of experimental runs. **Table** 4.4 shows the arrangement of L_{16}.

Table 4-4 L16 orthogonal array arrangement with input parameters

Expt. Run	**Experimental settings**					
	Part thickness	**Taper Angle**	**Pulse Duration**	**Discharge Current**	**Wire Speed**	**Wire Tension**
1	10	10	20	16	90	14
2	10	10	20	18	90	16
3	10	10	25	16	105	14
4	10	10	25	18	105	16
5	10	20	20	16	105	16
6	10	20	20	18	105	14
7	10	20	25	16	90	16
8	10	20	25	18	90	14
9	30	10	20	16	105	16
10	30	10	20	18	105	14
11	30	10	25	16	90	16
12	30	10	25	18	90	14
13	30	20	20	16	90	14
14	30	20	20	18	90	16
15	30	20	25	16	105	14
16	30	20	25	18	105	16

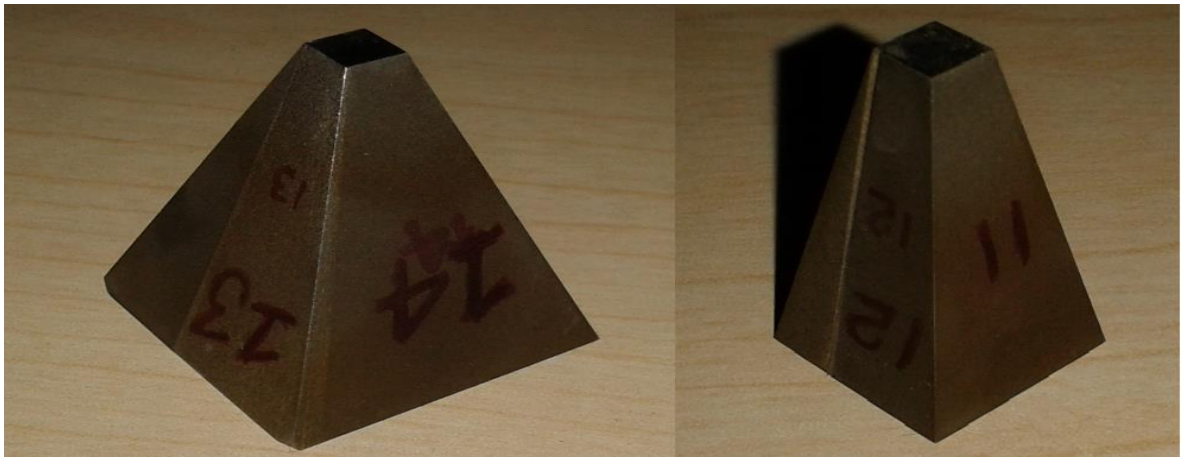

(a) (b)

Figure 4-2 AISI 316 Work samples after machining a). 20^0 taper angle and 30mm thickness b). 10^0 taper angle and 10mm thickness

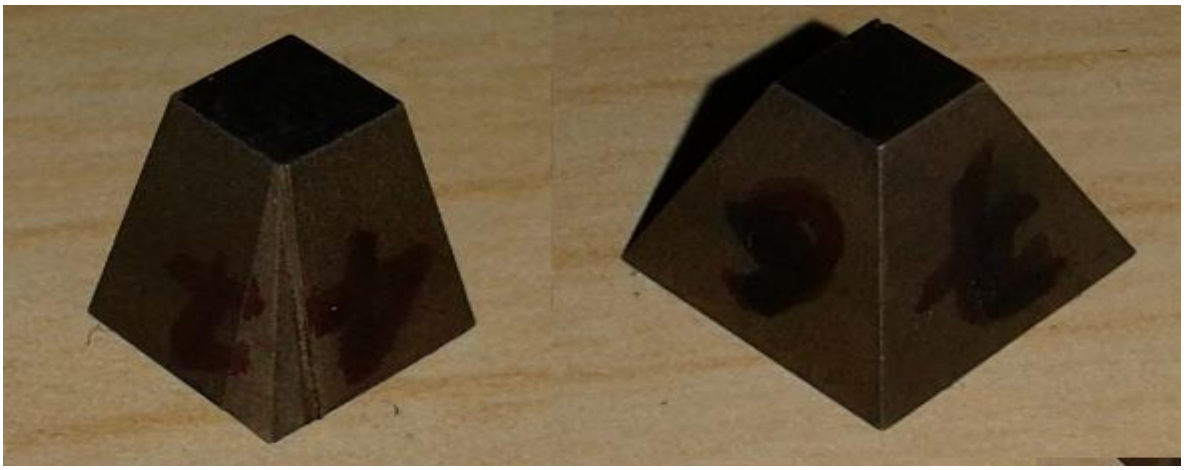

(a) (b)

Figure 4-3 AISI 316 Work samples after machining a). 10^0 taper angle and 10mm thickness b). 20^0 taper angle and 10mm thickness

The surface roughness value (in μm) has been obtained by measuring the mean absolute deviation, Ra (surface roughness) from the average surface level using SURTRONIC S128. The angular error can be expressed in minute and calculated by the following

Formula: Angular error = φ- θ

Where θ is the programmed angle or the angle expected in the machined part

φ is the actual angle obtained in the machined part due to the wire deformation as shown in Fig.

After machining, the angle of the inclined surface (φ) is measured with respect to the top surfaces using a Zeiss 850 CNC coordinate measuring machine.

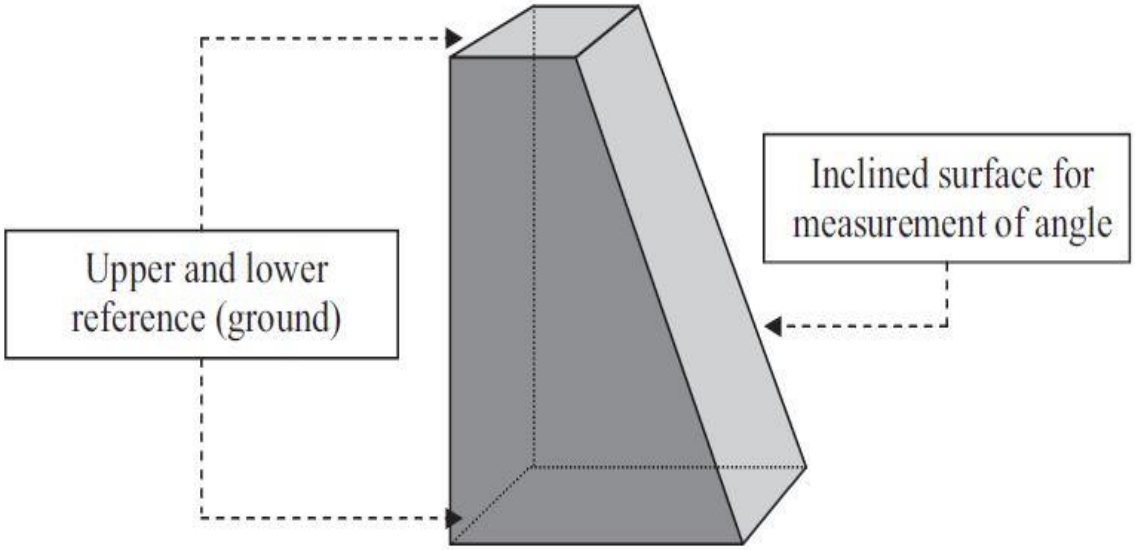

Figure 4-4 Geometry of the test part for measuring angular error in WEDM experiments

Figure 4-5 Taylor Hobson S125 AMETEK

For WEDM cutting speed is also a desirable characteristic and it should be as high as possible to give least machine cycle time leading to increased productivity. In the present study, cutting rate is a measure of job cutting which is digitally displayed on the screen of the machine and is given in mm/min. Surface roughness values (Ra) were measured using a Taylor Hobson S125 AMETEK Surtronic S – 125 roughness measuring instrument.

Table 4-5 Output responses

Expt. Run	Responses		
	Surface roughness	Cutting Speed	Angular error
1	2	1.8816	3.46
2	2.4	2.1504	3.1
3	2.5	2.5088	25.4
4	2.3	3.0106	6.36
5	2.3	3.5248	23.16
6	2.05	2.8198	8.59
7	2.25	2.2559	8.11
8	2.2	2.8198	7.19
9	2.33	1.7153	14.44
10	2.97	2.4299	2.18
11	2.37	1.1215	13.45
12	2.67	1.3254	5.12
13	2.5	1.1234	7.3
14	2.7	1.9875	1.32
15	2.5	1.4354	3.32
16	2.67	1.7225	4

Figure 4-6 ZEISS MC 850 Coordinate measuring machine for angular measurement

4.5 Utility Theory

In this project output responses surface roughness, cutting speed, and angular error was used for optimizing machining parameters of WEDM taper cutting process. The main aim is cutting speed should be maximum, surface roughness and angular error should be minimum. The utility can be defined as the usefulness of a product or a process in reference to the levels of expectations to the consumers. The performance evaluation of any machining process depends on a number of output

characteristics. Therefore, a combined measure is necessary to gauge its overall performance, which must take into account the relative contribution of all the quality characteristics. Such a composite index represents the overall utility of a product/process. It provides a methodological framework for the evaluation of alternative attributes made by individuals, firms and organizations. Utility refers to the satisfaction that each attribute provide to the decision maker. Thus, utility theory assumes that any decision is made on the basis of the utility maximization principle, according to which the best choice is the one that provides the highest satisfaction to the decision maker.

According to the utility theory if X_i is the measure of effectiveness of an attribute (or quality characteristics) i and there are n attributes evaluating the outcome space, then the joint utility function can be expressed as:

$$U(Z_1,Z_2,\ldots\ldots,Z_n) = f(U_1(Z_1),U_2(Z_2),\ldots\ldots\ldots\ldots U_n(Z_n)) \ldots\ldots\ldots\ldots (1)$$

Where $U_i(Z_i)$ represents the utility function of the i^{th} attribute. The total utility value of any attribute should be calculated as the summation of each utility value for all the responses and can be written as

$$U(Z_1,Z_2,\ldots\ldots,Z_n) = \sum_{i=1}^{n} U_i(Z_i) \ldots\ldots\ldots\ldots\ldots\ldots\ldots\ldots\ldots\ldots (2)$$

Some value of weight is assigned to each attribute according to their importance so that the summation of all the weights is equal to 1

$$U(Z_1,Z_2,\ldots\ldots,Z_n) = \sum_{i=1}^{n} W_i U_i(Z_i) \ldots\ldots\ldots\ldots\ldots\ldots\ldots\ldots\ldots\ldots (3)$$

Here W_i represents the weight assigned to the i^{th} response. A preference no. is set for each response to determine the utility value for each response. Two random preference numbers 0 and 9 are allotted to just acceptable and the best value of the response respectively. The preference no. for the i^{th} response can be written on a logarithmic scale as follows:

$$P_i = AX \log\left(\frac{Z_i}{Z_i^{'}}\right) \ldots\ldots\ldots\ldots\ldots\ldots\ldots\ldots\ldots\ldots\ldots\ldots\ldots\ldots (4)$$

Where Z_i represents i^{th} response and $Z_i^{'}$ is the just acceptable value of the response. Just acceptable value is the minimum or maximum value of the response depending upon we want to maximize or minimize it respectively. Where the value of the constant A is calculated by the equation as

$$A = \frac{9}{\log(\frac{Z^*}{Z_i})} \quad \text{..... (5)}$$

Here Z^* is the best value. When $Z_i = Z^*$, $P_i = 9$.

Table 4-6 Utility value of individual responses

Expt. Run	Utility factor for responses			Final Utility Factor
	Surface roughness	Cutting Speed	Angular error	
1	9	4.06678	6.06717	6.377982
2	4.850195	5.11623	6.40155	5.455989
3	3.92105	6.32773	0	3.416259
4	5.818891	7.76073	4.2144	5.931342
5	5.818891	9	0.28098	5.033292
6	8.437973	7.24616	3.29962	6.327917
7	6.319151	5.49264	3.47462	5.095472
8	6.830653	7.24616	3.84108	5.972631
9	5.523929	3.33953	1.71881	3.527424
10	0	6.07659	7.4731	4.516562
11	5.1365	0	1.93497	2.357156
12	2.423661	1.31286	4.87446	2.870326
13	3.92105	0.0133	3.79487	2.576407
14	2.169346	4.49711	9	5.222152
15	3.92105	1.93946	6.19288	4.017796
16	2.423661	3.37245	5.62578	3.807298

Raw R-square (1-Residual/Total) 0.979

Regression equation is used for prediction.

$Z= - (A_0*x(1)^A_1*x(2)^A_2*x(3)^A_3*x(4)^A_4*x(5)^A_5*x(6)^A_6)$ …… (6)

Table 4-6

Table4-7 Parameter Estimates

Parameter	Estimate	ASE	Parameter/ASE	Wald 95% Confidence Interval	
				Lower	Upper
A0	0.542	2.488	0.218	-5.086	6.169
A1	-0.366	0.096	-3.806	-0.583	-0.148
A2	0.124	0.142	0.872	-0.197	0.445
A3	-0.623	0.442	-1.411	-1.622	0.376
A4	1.724	0.846	2.039	-0.189	3.638
A5	-0.056	0.634	-0.088	-1.491	1.379
A6	0.045	0.733	0.061	-1.614	1.704

z= - (0.542*(x(1)^-0.366)*(x(2)^0.124)*(x(3)^-0.623)*(x(4)^1.724)*(x(5)^-0.056)*

(x(6)^0.045)) ……...…… (7)

Chapter 5

Result and Discussion

5 Result and Discussions

Brass wire is passing continuously through the fixed guides with an inclination 10^0 and 20^0 and is heavily loaded, due to this stresses has been occurring between wire and guide. Different stress at different tensions was tabulated below.

Table 5-1 Different contact stresses at different wire position and tension

S No	Wire Length	Angle	Tension	Equivalent Stress	Max. Principal Stress	Normal Stress	Shear Stress
1	5	10	14	382.81	298.21	14.227	51.36
2	5	10	16	403.49	338.33	18.504	57.621
3	5	20	14	351.7	296.64	36.471	100.47
4	5	20	16	396.87	339.14	39.348	112.96
5	10	10	14	387.28	299.01	20.503	53.175
6	10	10	16	384.58	297.42	26.868	50.178
7	10	20	14	388.68	311.17	54.976	97.294
8	10	20	16	404.62	337.18	45.66	114.72
9	15	10	14	376.81	304.13	12.122	50.716
10	15	10	16	422.51	351.85	16.505	57.44
11	15	20	14	336.19	296.22	36.719	96.025
12	15	20	16	394.48	335.05	39.694	111.07

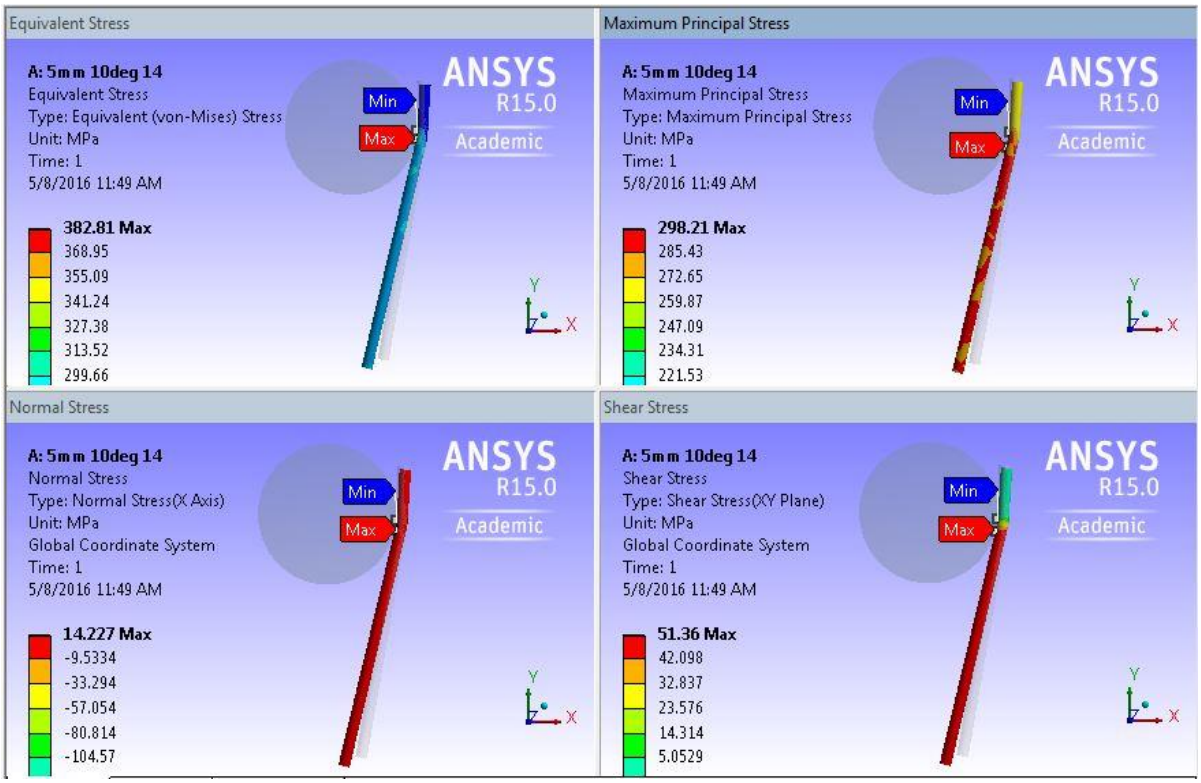

Figure 5-1 Contact stresses result of 5mm wire inclined at 10deg applied tension 14N

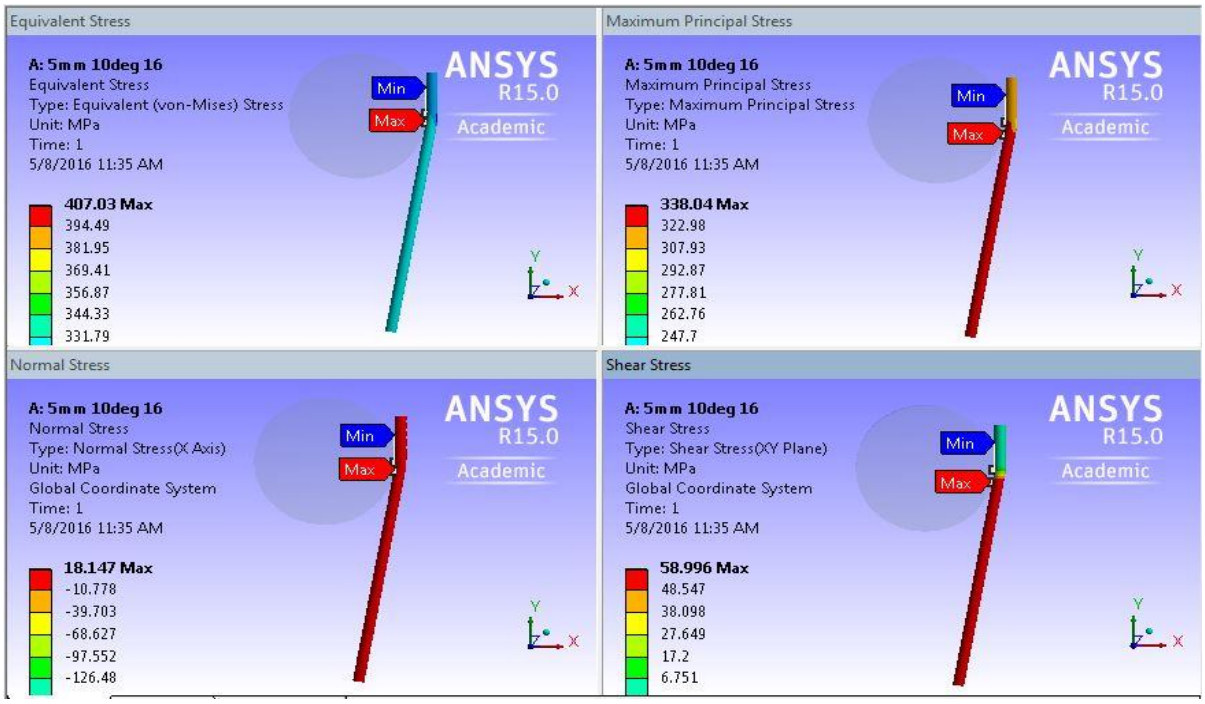

Figure 5-2 Contact stresses result of 5mm wire inclined at 10deg applied tension 16N

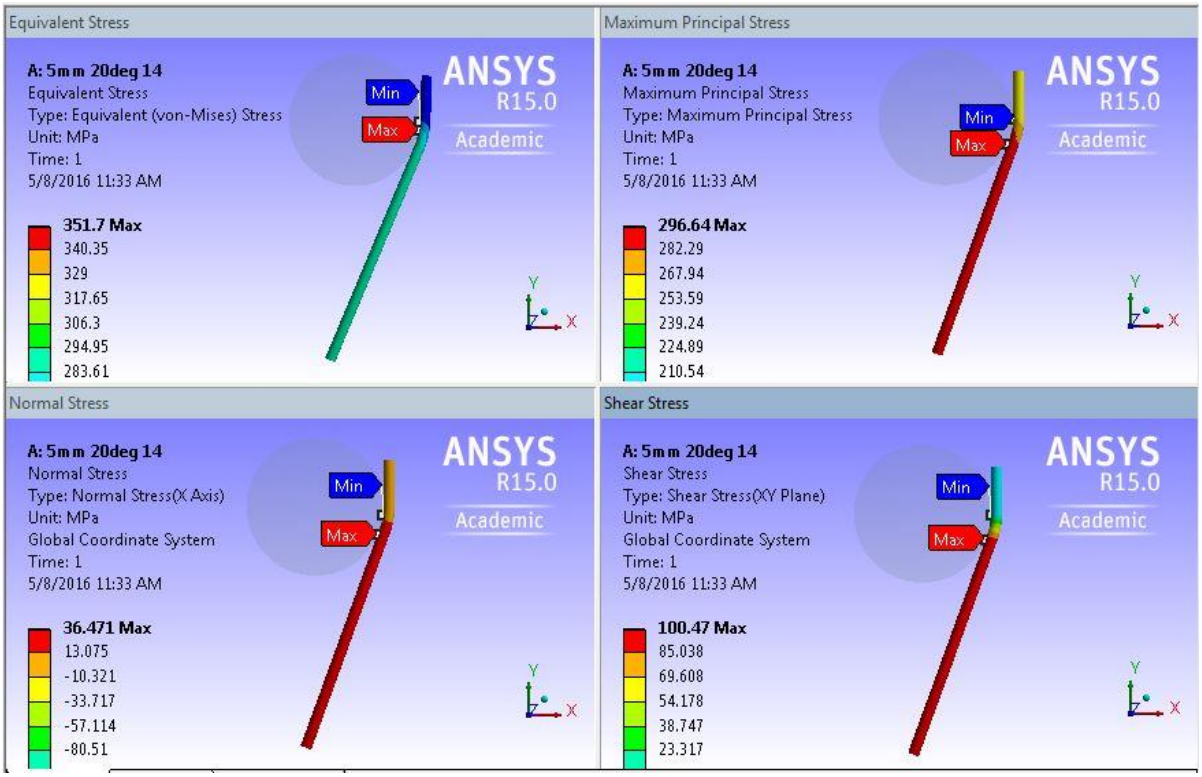

Figure 5-3 Contact stresses result of 5mm wire inclined at 20deg applied tension 14N

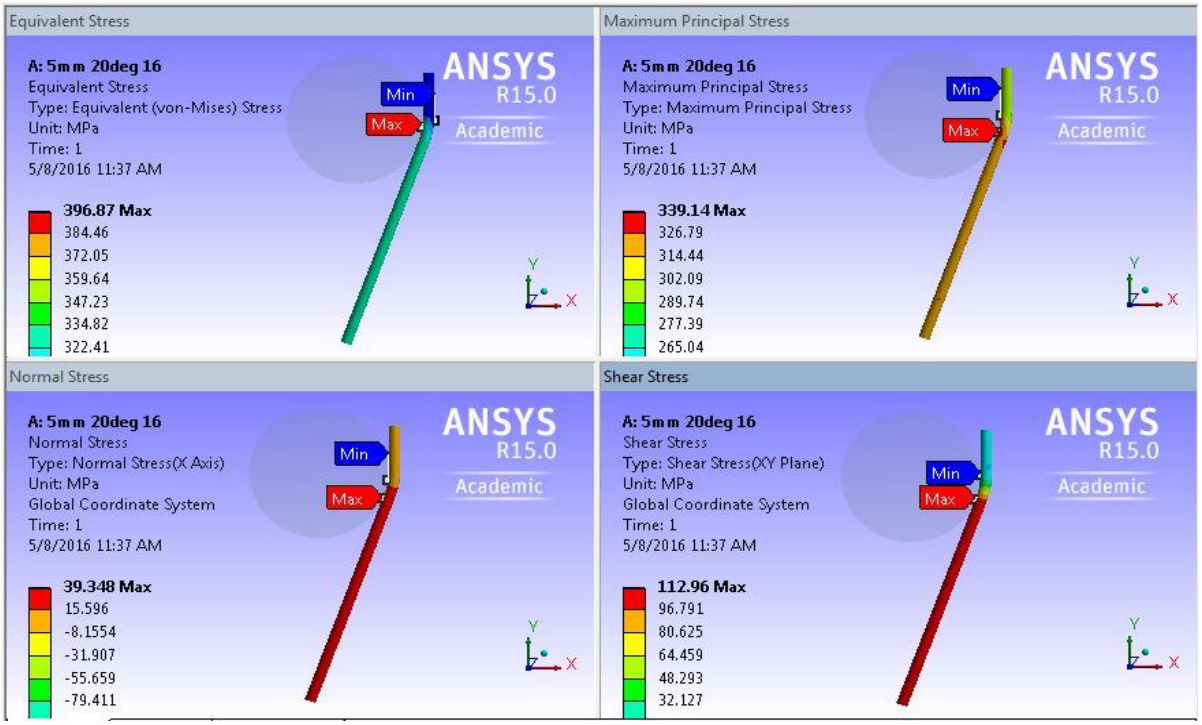

Figure 5-4 Contact stresses result of 5mm wire inclined at 20deg applied tension 16N

Figure 5-5 Contact stresses result of 10mm wire inclined at 10deg applied tension 14N

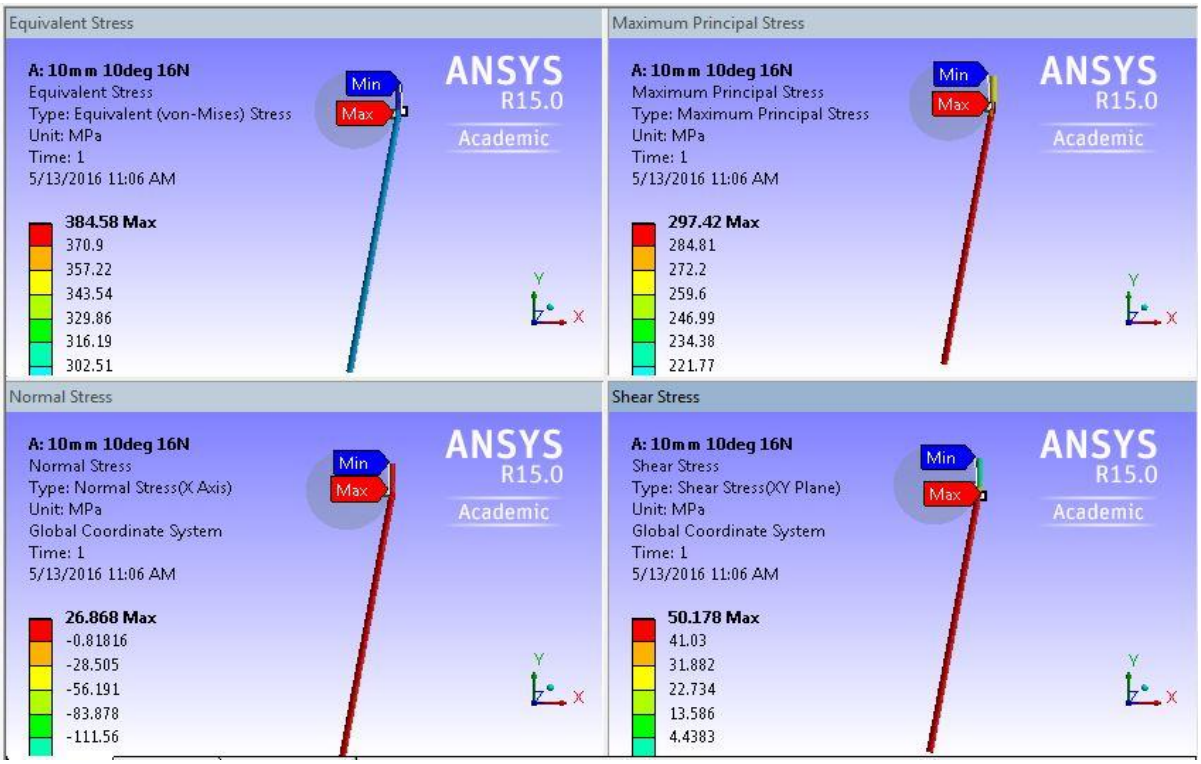

Figure 5-6 Contact stresses result of 10mm wire inclined at 10deg applied tension 16N

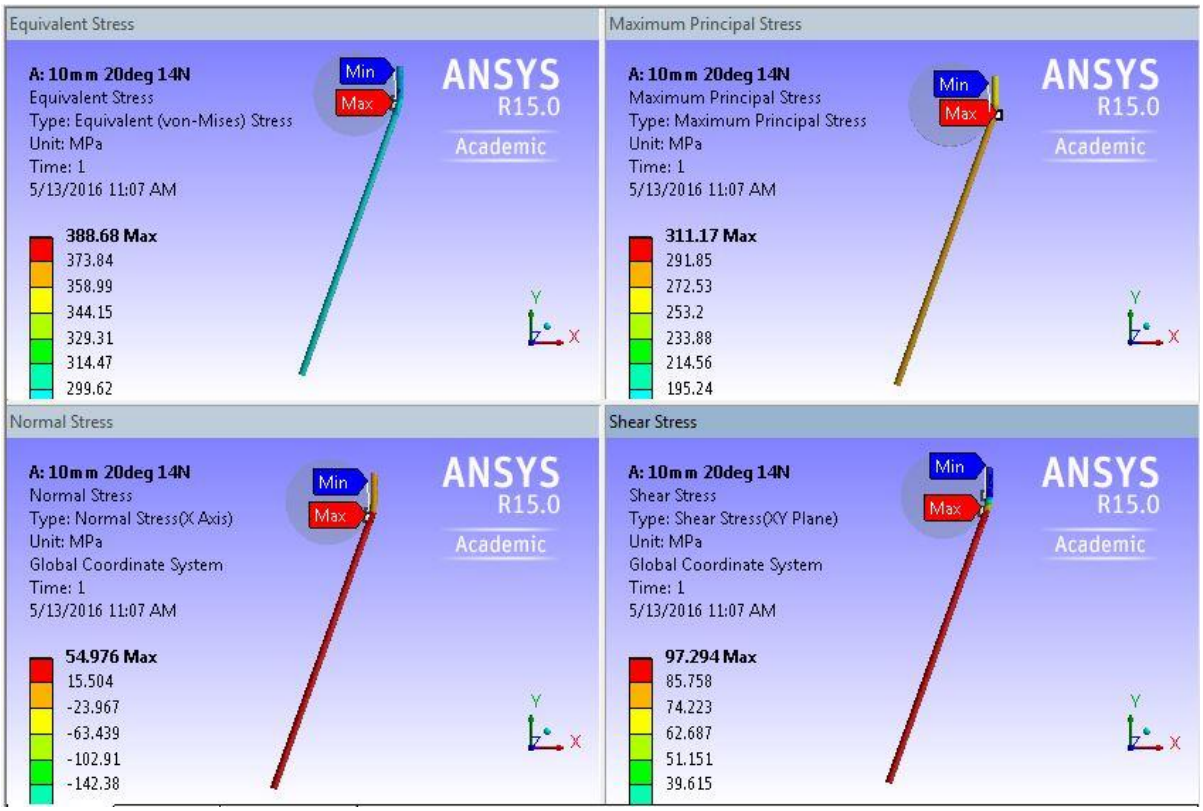

Figure 5-7 Contact stresses result of 10mm wire inclined at 20deg applied tension 14N

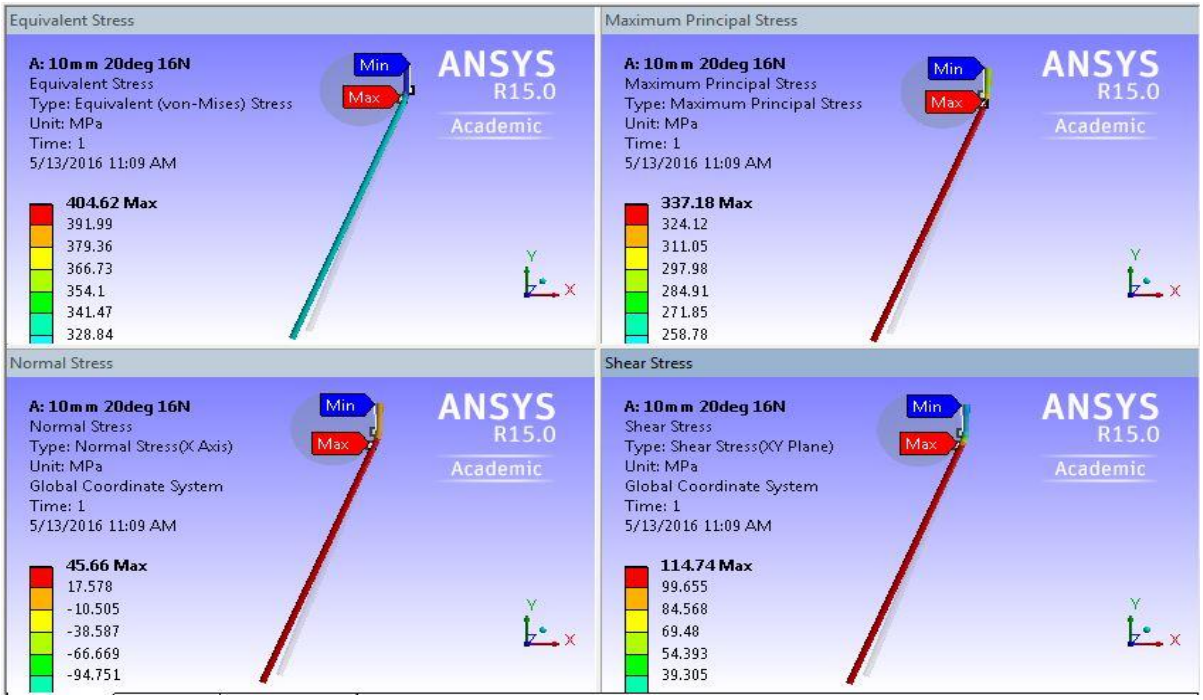

Figure 5-8 Contact stresses result of 10mm wire inclined at 20deg applied tension 16N

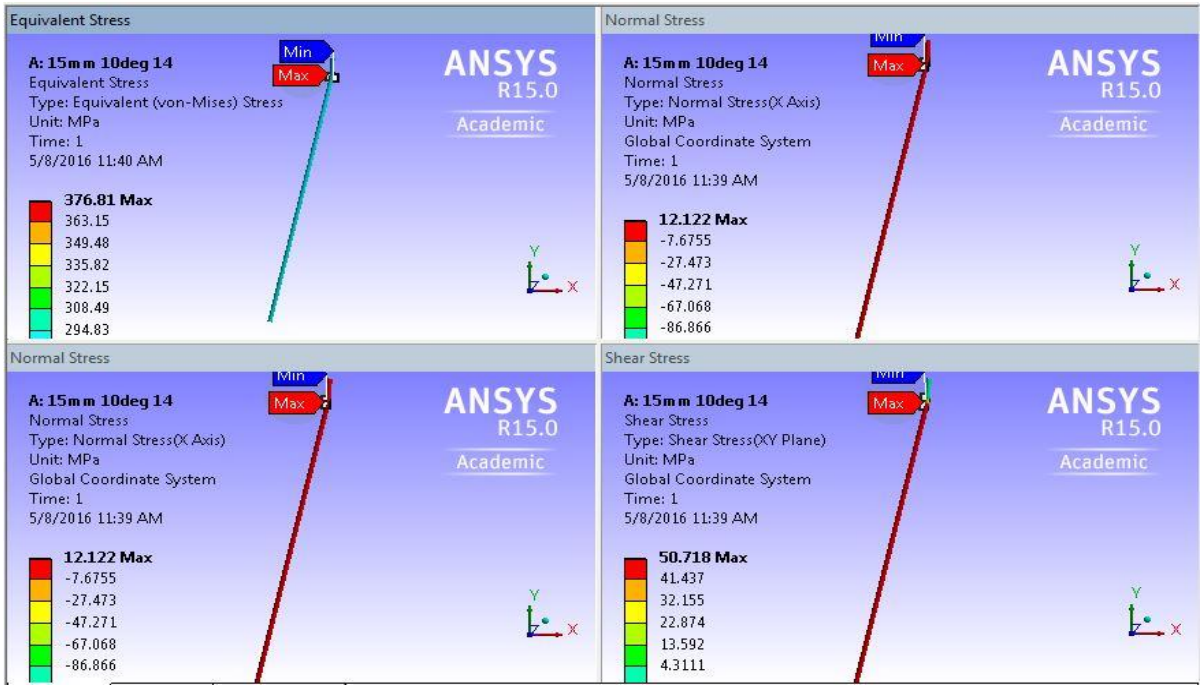

Figure 5-9 Contact stresses result of 15mm wire inclined at 10deg applied tension 14N

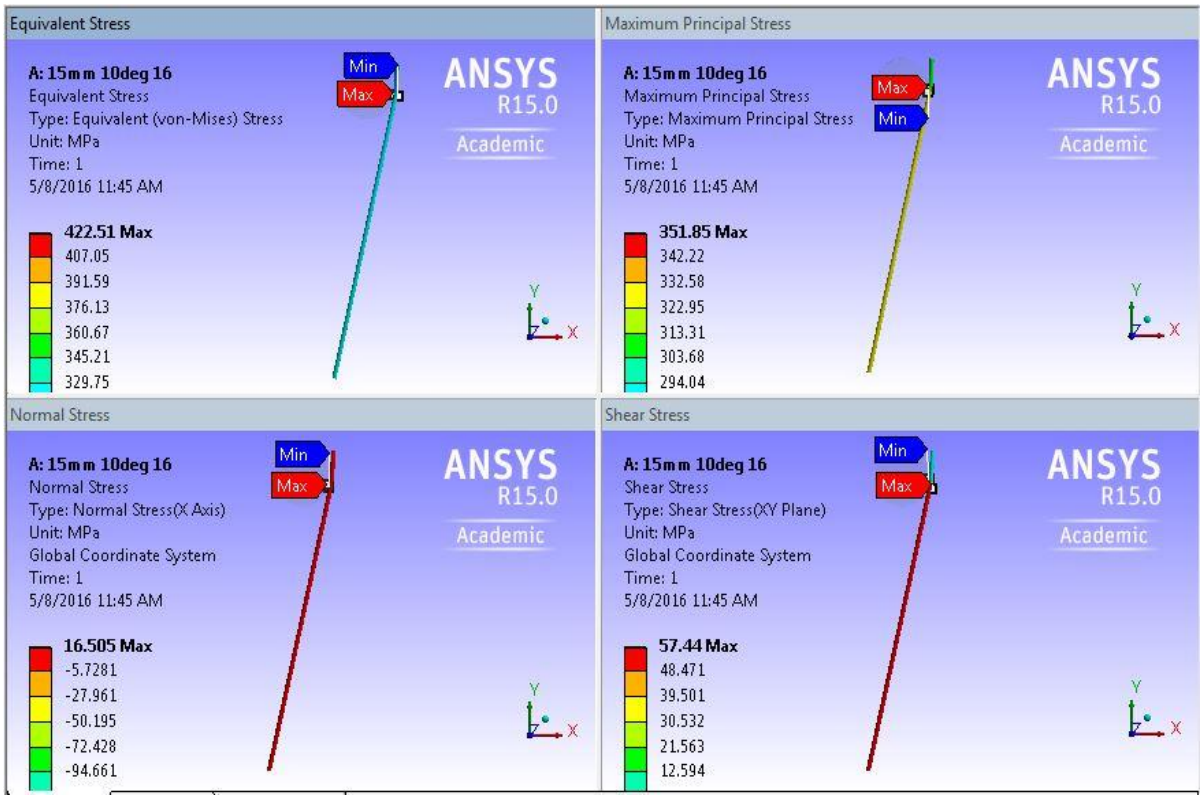

Figure 5-10 Contact stresses result of 15mm wire inclined at 10deg applied tension 16N

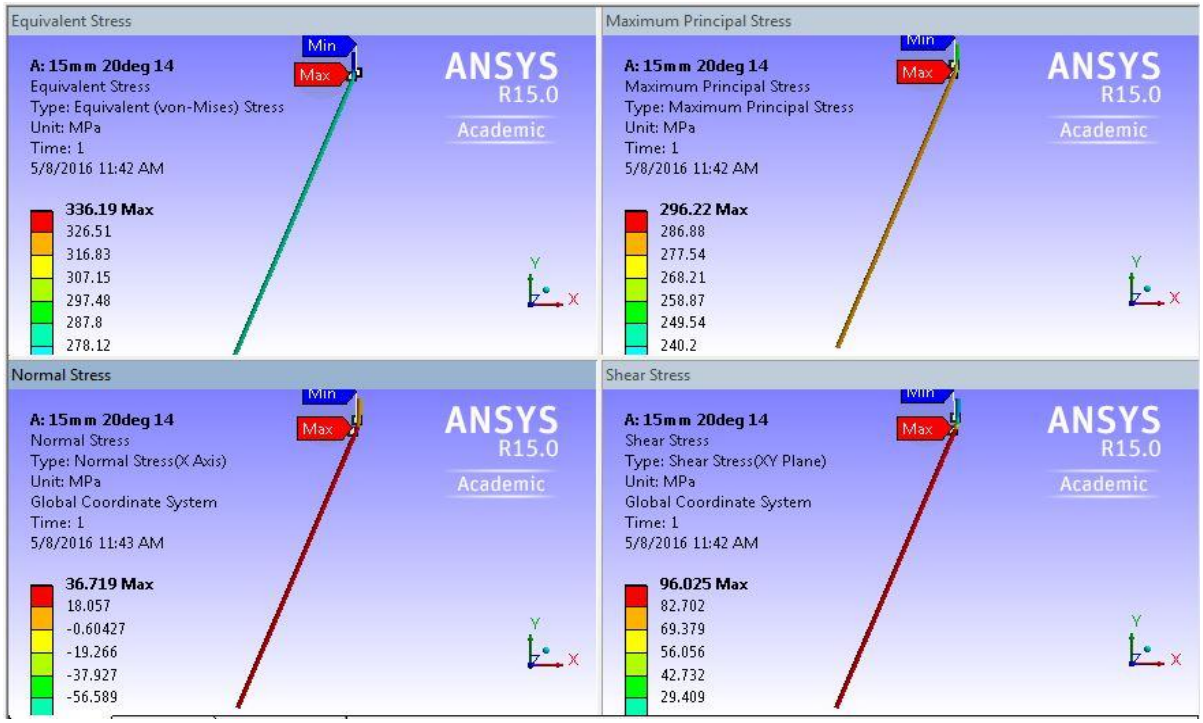

Figure 5-11 Contact stresses result of 15mm wire inclined at 20deg applied tension 14N

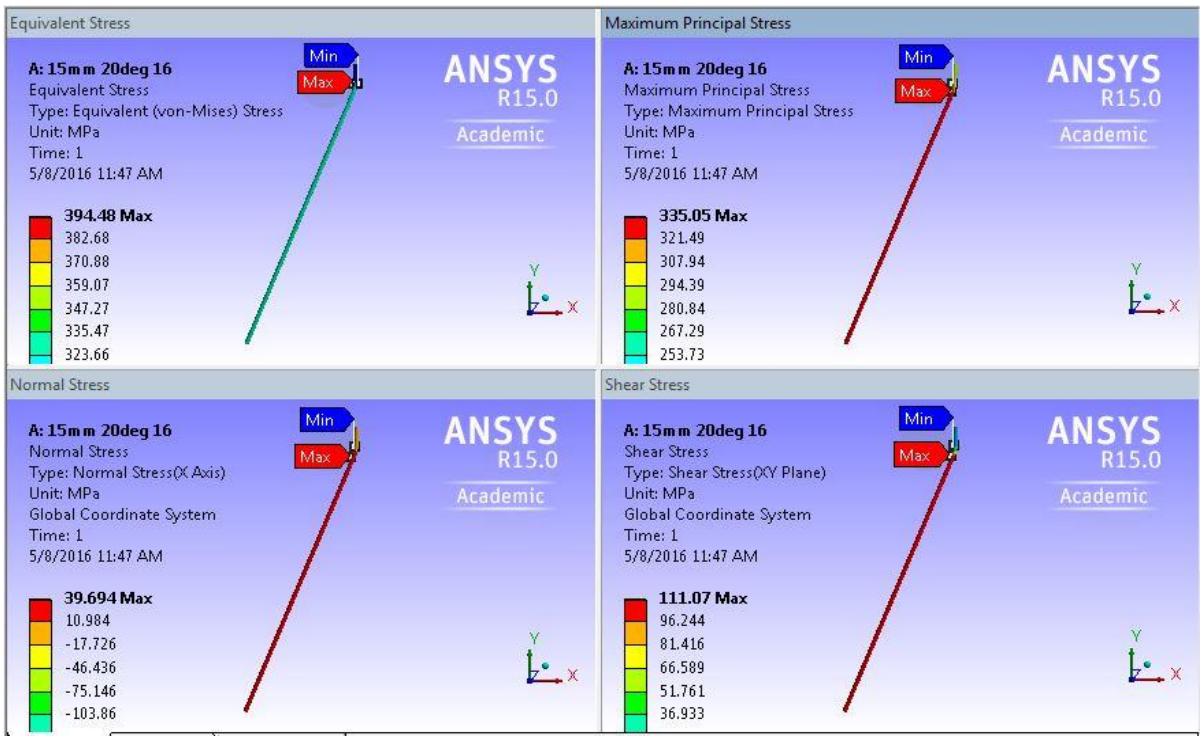

Figure 5-12 Contact stresses result of 15mm wire inclined at 20deg applied tension 16N

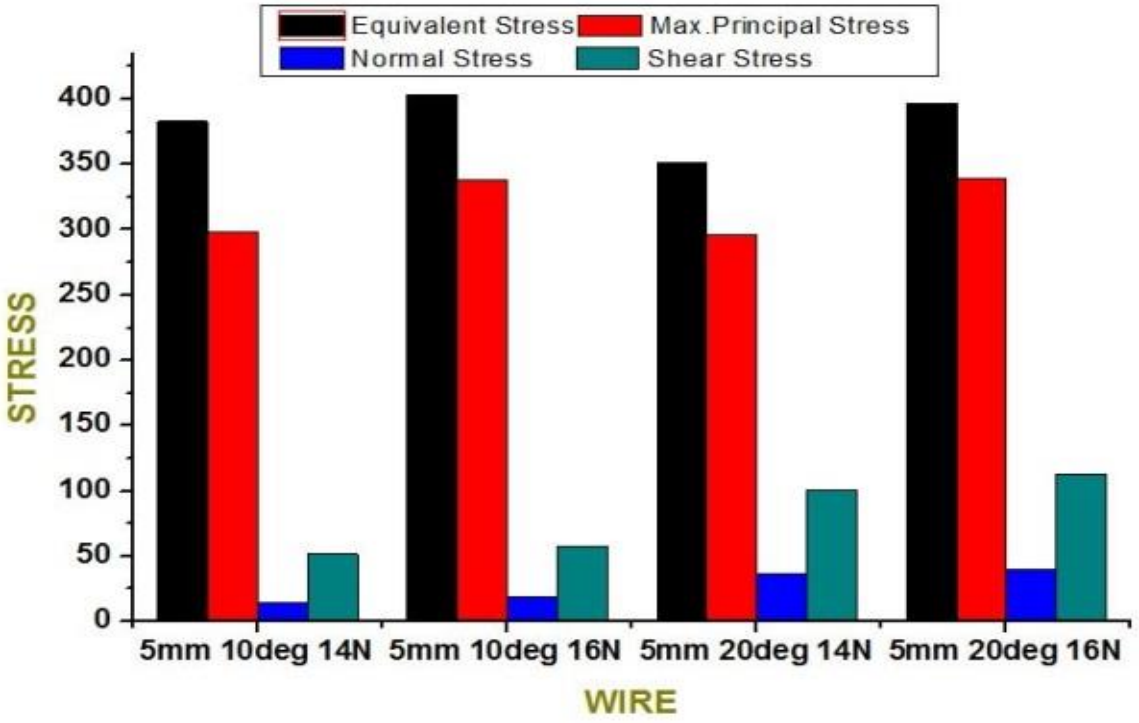

Figure 5-13 Contact stresses of 5mm length wire at 10^0 & 20^0 and 14N & 16N

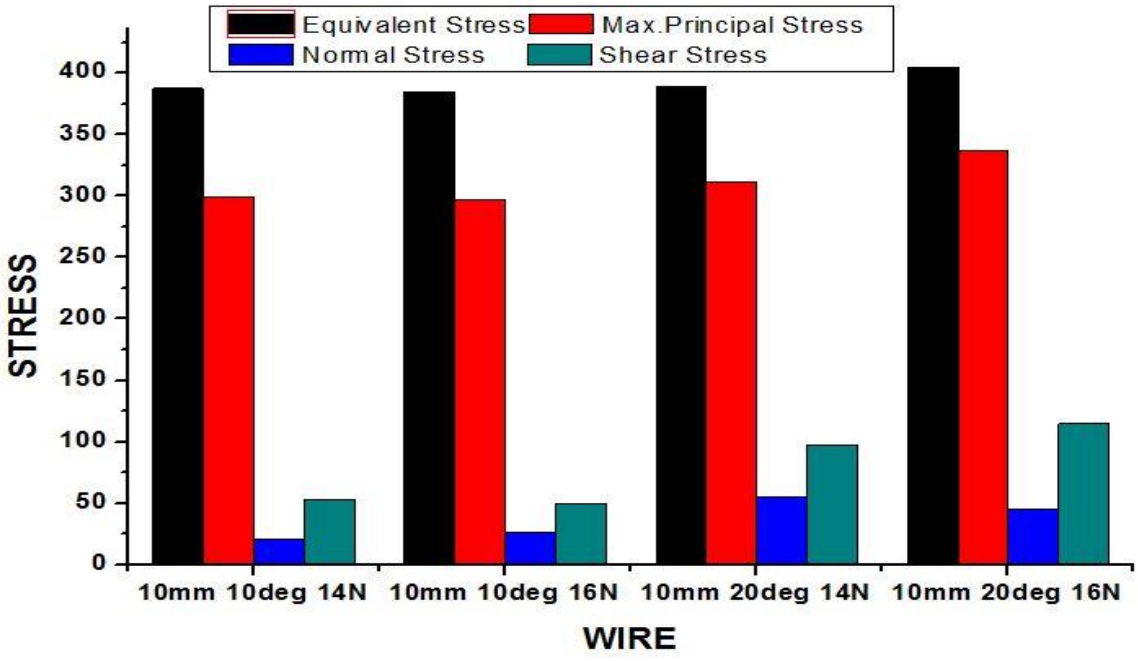

Figure 5-14 Contact stresses of 10mm length wire at 10^0 & 20^0 and 14N & 16N

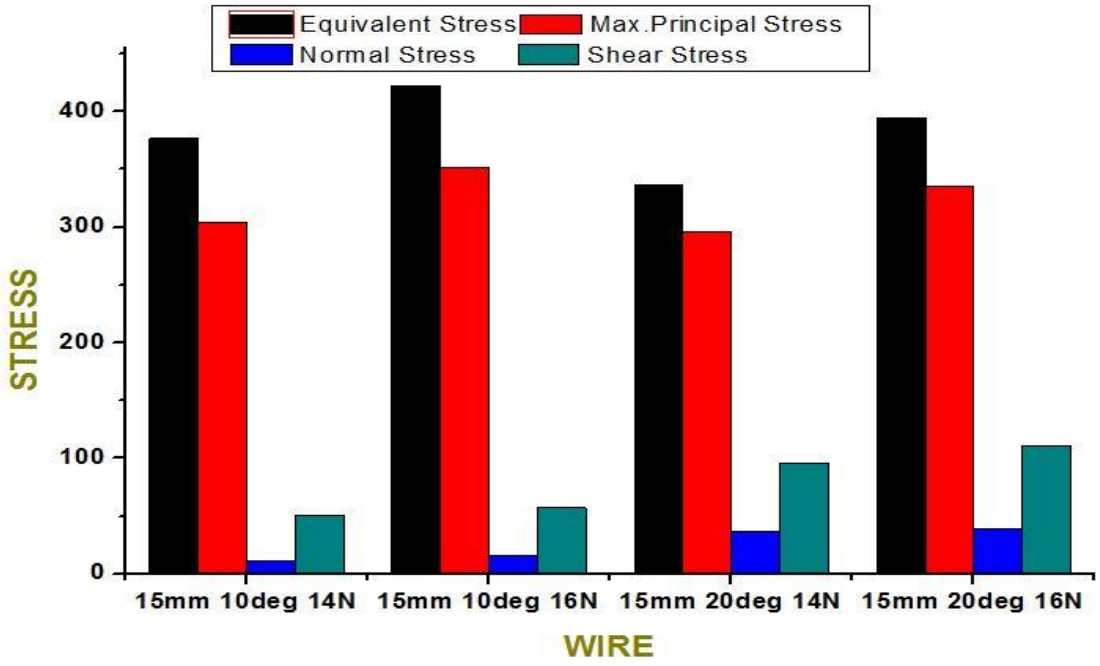

Figure 5-15 Contact stresses of 15mm length wire at 10^0 & 20^0 and 14N & 16N

Table 5-2 Angular error results using Finite element analysis at different wire positions

S No	Wire			Directional Deformation	Angle (Degree)	Angle	Error (%)
	Length (mm)	Angle (Deg)	Tension (N)			D M S	
1	5	10	14	0.034576	10.4026	10 24 09	4.026
2	5	10	16	0.01071	10.1242	10 07 27	1.242
3	5	20	14	0.018437	20.2249	20 13 29	2.249
4	5	20	16	0.013197	20.161	20 09 39	1.619
5	10	10	14	0.045821	10.2667	10 16 00	2.667
6	10	10	16	0.053787	10.3133	10 18 47	3.133
7	10	20	14	0.028327	20.1512	20 09 04	1.512
8	10	20	16	0.040464	20.2471	20 14 49	2.471
9	15	10	14	0.06345	10.2463	10 14 46	2.463
10	15	10	16	0.063218	10.2453	10 14 43	2.453
11	15	20	14	0.032101	20.1305	20 07 49	1.305
12	15	20	16	0.047281	20.1923	20 11 32	1.923

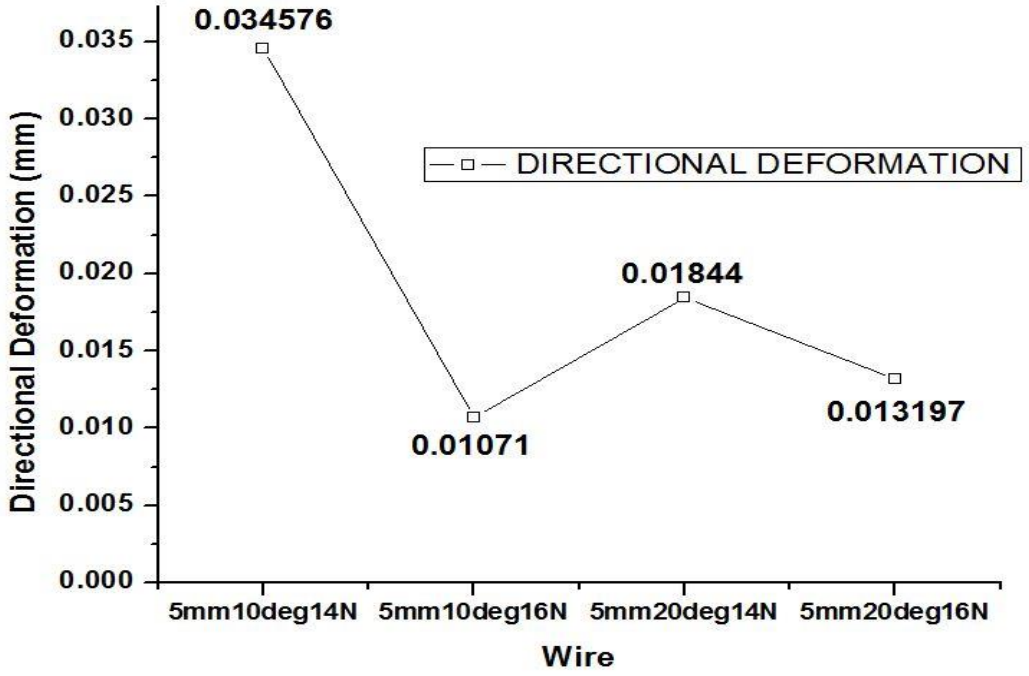

Figure 5-16 Directional deformation of wire length 5mm at 10^0 & 20^0 and 14N & 16N

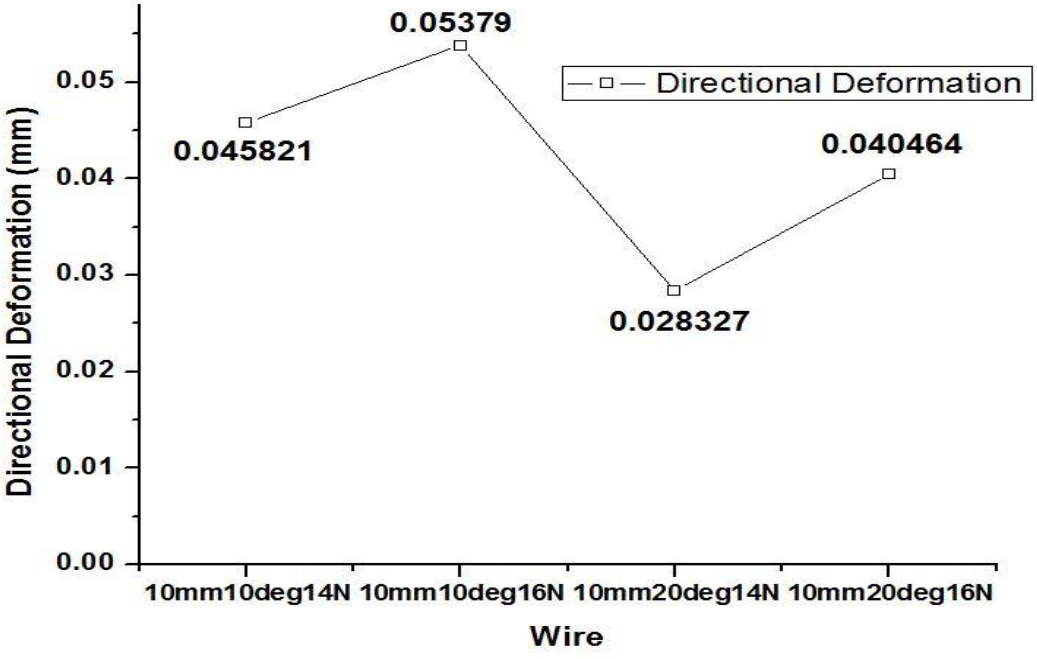

Figure 5-17 Directional deformation of wire length 10mm at 10^0 & 20^0 and 14N & 16N

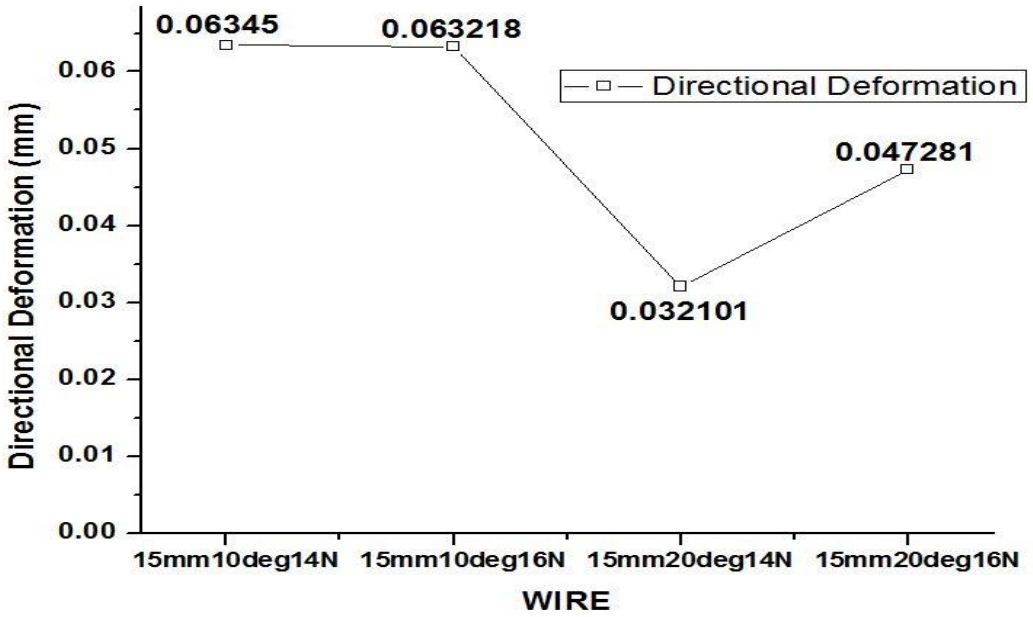

Figure 5-18 Directional deformation of wire length 15mm at 10^0 & 20^0 and 14N & 16N

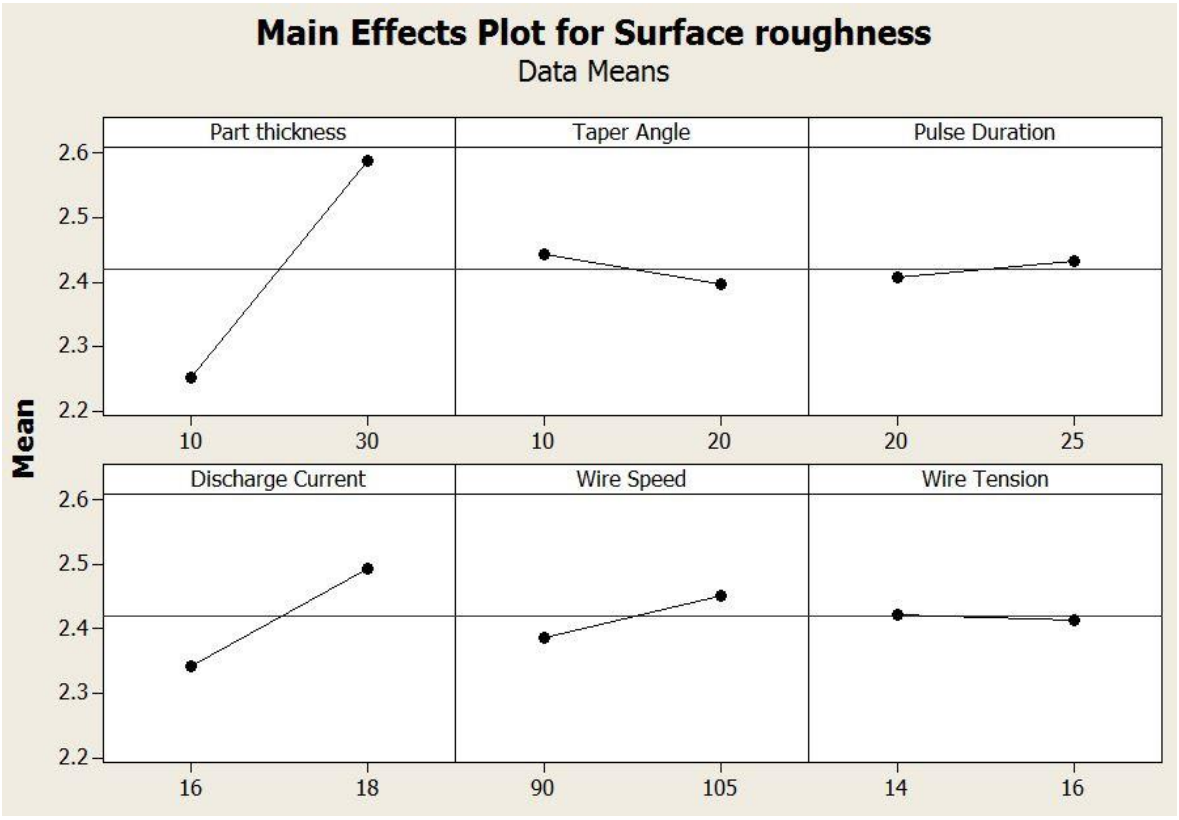

Figure 5-19 Main effects plot for Surface roughness

From figure 5.19, by increasing, part thickness from 10mm to 30mm, pulse duration from 20µs to 25µs, discharge current 16Amp to 18Amp and wire speed from 90mm/s to 105 mm/s surface roughness increases.

Surface roughness reduces by increasing, taper angle from 10^0 to 20^0 and wire tension from 14N to 16N.

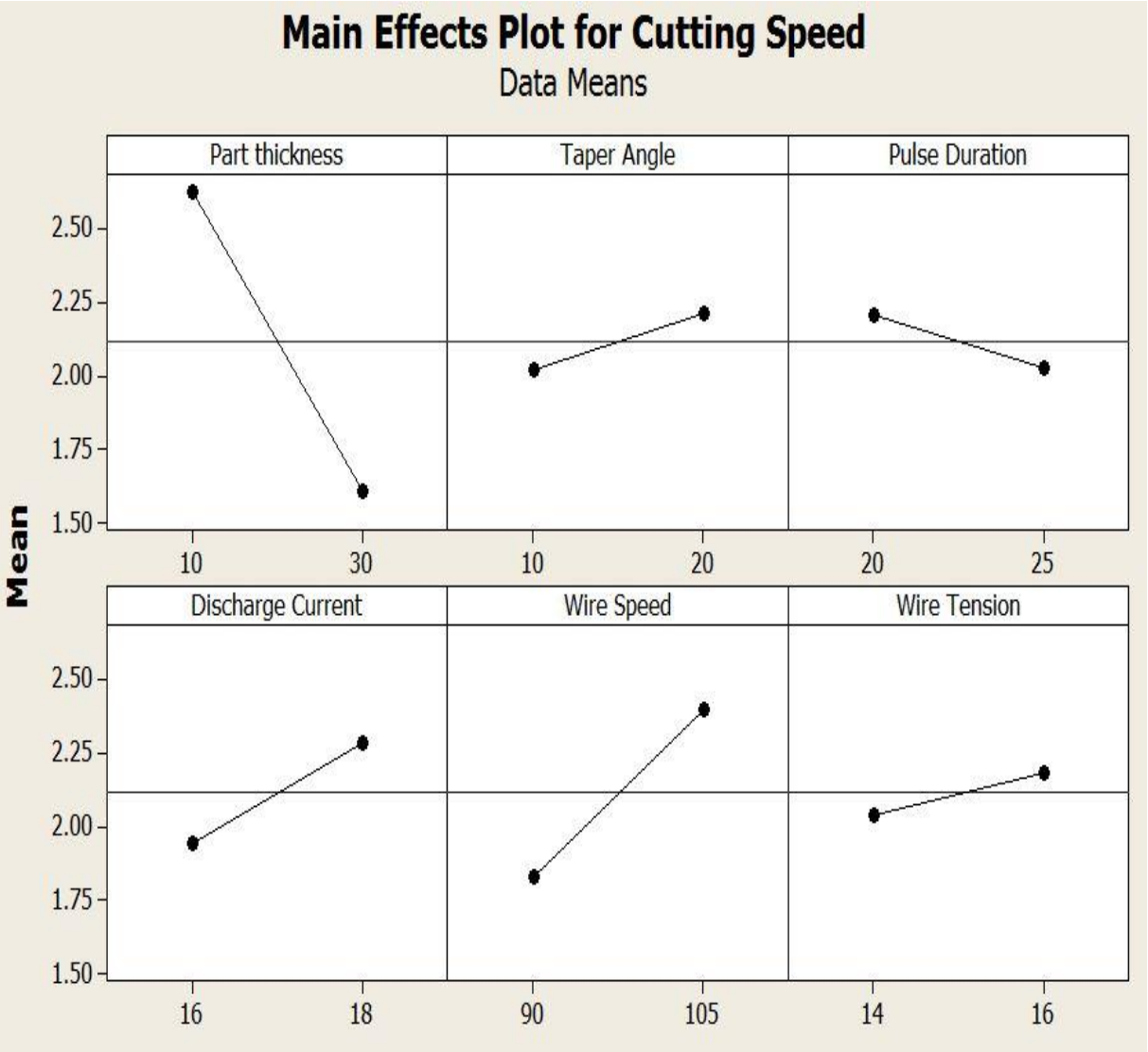

Figure 5-20 Main effects plot for Cutting speed

From figure 5.20 by increasing taper angle from 10^0 to 20^0 , discharge current from 16Amp to 18Amp, wire speed from 90mm/s to 105 mm/s, and wire tension from 14N to 16N cutting speed increases.

Cutting speed reduces by increasing, part thickness from 10mm to 30mm and pulse duration from 20µs to 25µs

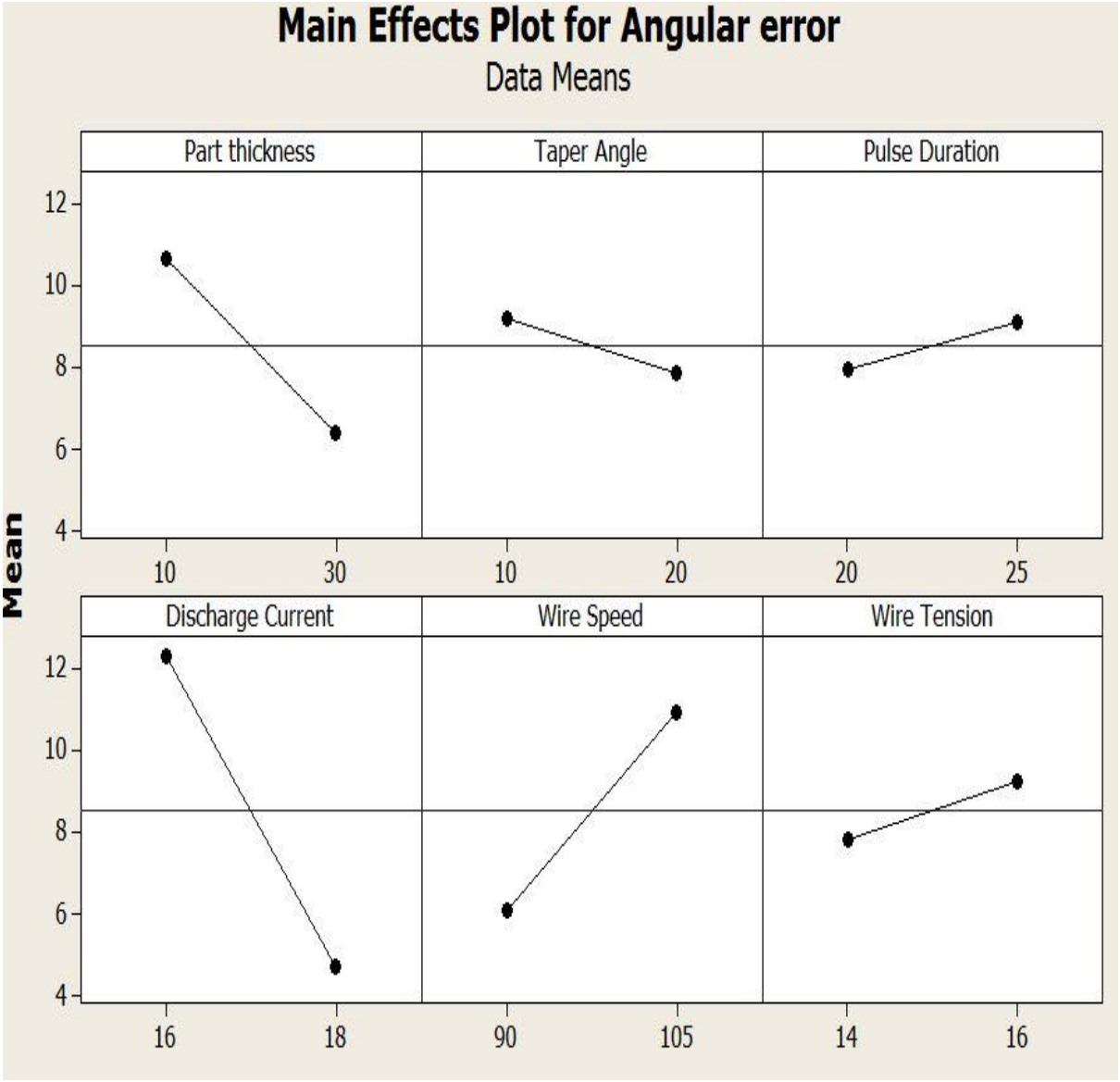

Figure 5-21 Main effects plot for Angular error

From figure 5.21 by increasing pulse duration from 20μs to 25μs, wire speed from 90mm/s to 105 mm/s, and wire tension from 14N to 16N Angular error increases.

Angular error reduces by increasing, part thickness from 10mm to 30mm, taper angle from 10^0 to 20^0 , and discharge current from 16Amp to 18Amp.

5.1 Comparison between FEM Analyses vs. Experimental Analysis

A. FEM analysis

1. An angular error has been reduced by increasing machining taper angle from 10^0 to 20^0. This means, at low machining angle high angular errors and at high machining angle less angular error is noticed.

2. The deviations with respect to the programmed value of the angle range from 7′49″, in the case of parts of thickness 30 mm and angle 20°, to 24′09″ in the case of parts of thickness 10 mm and angle 10°.

3. Contact stresses, equivalent stress and maximum principal stresses between wire and guide have been reduced gradually by increasing taper angle and tension; contact stresses, normal stress, and shear stresses between wire and guide has been increasing gradually by increasing taper angle and tension.

Table 5-3 Results of angular error predicted by FEM analysis, compared to experimental tests

	Finite Element Analysis	Experimental Analysis
Angular error	10^0 to 20^0 decreases	10^0 to 20^0 decreases
10mm & 10^0 angle	24′09″	31′46″
10mm & 20^0 angle	13′29″	23′16″
30mm &10^0 angle	14′46″	14′44″
30mm & 20^0 angle	7′49″	7′03″

B. Experimental analysis

1. The angular error obtained after applying this method is within the range from 1′32″ for the case of part thickness 30 mm and angle 20°, to 25′4″for the case of part thickness 10 mm and angle 10°.

2. In 75% of results obtained from the three models proposed, the angular deviation is below 9′.

3. The below figure 5.22 representing the no. of iterations to the fitness value, and the final point represented the parameter setting, like this: part thickness=10mm, taper angle = 19.9940958^0 pulse discharge=20.341µs, discharge current = 17.9995765Amp, wire speed=100.268454 mm/min, wire tension =15.9713N; Objective function value = 6.612306653076921.

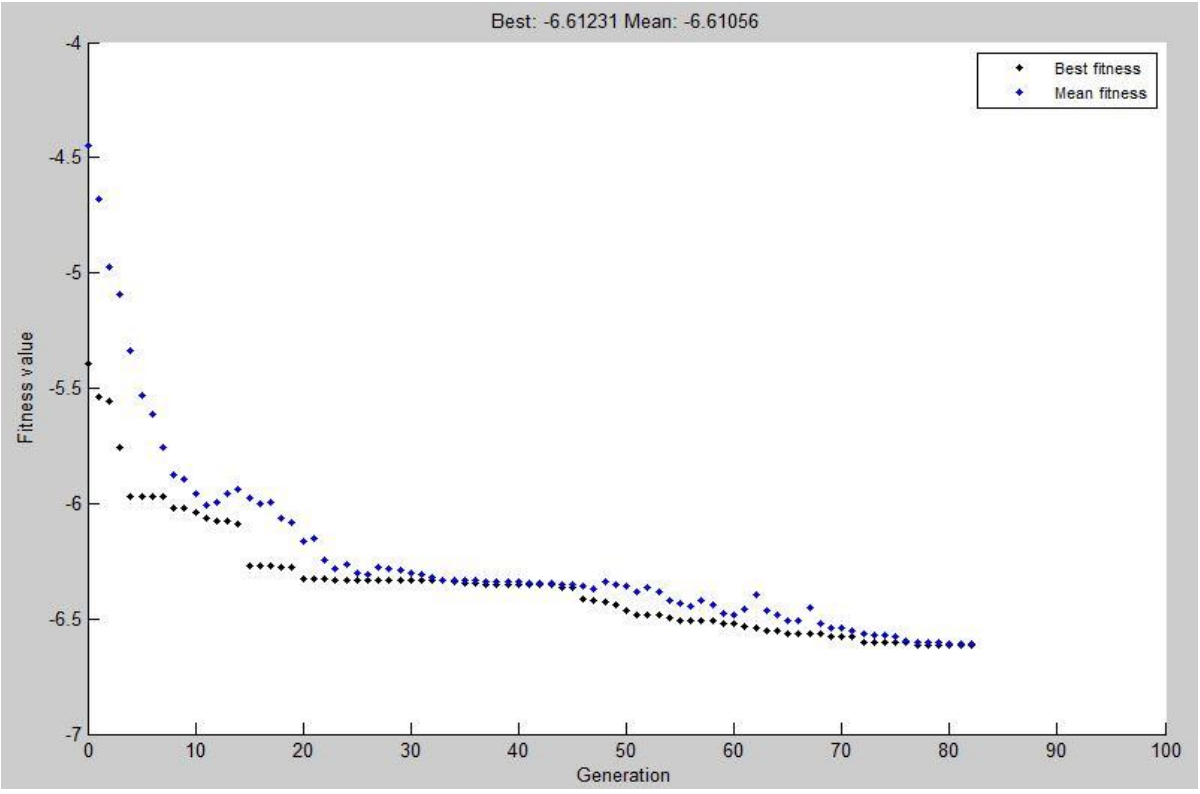

Figure 5-22 Mean and Best fitness graph, total no. of iterations 82

Chapter 6

Conclusion

Conclusion

The project proposes a systematic study of the effect of process parameters on various performance characteristics such as angular error, surface roughness, and cutting speed using Taguchi's L_{16} experimental design. Part thickness, taper angle, pulse duration, discharge current, wire speed and wire tension has been considered as the input parameters in the study. Numerical analysis carried out using finite element analysis (FEA) to find the angular error by changing wire position and wire tension.

Taper cutting operation is a major concern among the tool engineers while producing tools and dies for complex parts involving tight corners, deep slots and feature at multiple angles using wire electrical discharge machining process. The proposed approach can effectively assist engineers in determining the optimal process parameter setting for simultaneously minimizing the angular error, surface roughness, and maximizing cutting rate during taper cutting operation using WEDM.

1. The effect of process parameters like Part thickness, taper angle, pulse duration, discharge current, wire speed, and wire tension have been considered in the study. From the analysis, it was concluded that most of the influence is due to the part thickness and angle, which determine wire's mechanical behavior, the influence of the EDM parameters on the angular error being smaller.

2. When compared with industrial practice, based on trial-and- error experiments, the models proposed here are more general and permit a deeper insight into the scientific knowledge of the problem. In the case of the numerical model, the results set the basis for future research of new guide geometries and new generations of wires.

3. Utility concept is efficient to solve a multi-response optimization problem. This approach has the capability of including more number of quality characteristics and process parameters. The predictive equations for overall utility index relating to the process parameters have been successfully developed and confirmation experiments are also carried out to validate the models.

Bibliography

1. Ho, K.H., Newman, S.T., Rahimifard, S. and Allen, R.D., 2004. State of the art in wire electrical discharge machining (WEDM). International Journal of Machine Tools and Manufacture, 44(12), pp.1247-1259.
2. Dauw, D.F. and Beltrami, I., 1994. High-precision wire-EDM by online wire positioning control. CIRP Annals-Manufacturing Technology, 43(1), pp.193-197.
3. Dauw, D.F., Sthioul, H., Delpretti, R. and Tricarico, C., 1989. Wire analysis and control for precision EDM cutting. CIRP Annals-Manufacturing Technology, 38(1), pp.191-194.
4. Kinoshita, N., Fukui, M. and Kimura, Y., 1984. Study on wire-EDM: inprocess measurement of mechanical behaviour of electrode-wire. CIRP Annals-Manufacturing Technology, 33(1), pp.89-92.
5. Yan, M.T. and Huang, P.H., 2004. Accuracy improvement of wire-EDM by real-time wire tension control. International Journal of Machine Tools and Manufacture, 44(7), pp.807-814.
6. Wang, J. and Ravani, B., 2003. Computer aided contouring operation for traveling wire electric discharge machining (EDM). Computer-Aided Design, 35(10), pp.925-934.
7. Sarkar, S., Sekh, M., Mitra, S. and Bhattacharyya, B., 2011. A novel method of determination of wire lags for enhanced profile accuracy in WEDM. Precision Engineering, 35(2), pp.339-347.
8. Rana, R., Mani, A., Kochhar, A., Wadhwa, S., Daiya, S.K., Taliyan, S. and Lal, R., An Overview on Process Parameters Improvement in Wire Electrical Discharge Machining.
9. Rana, R., Mani, A., Kochhar, A., Wadhwa, S., Daiya, S.K., Taliyan, S. and Lal, R., An Overview on Process Parameters Improvement in Wire Electrical Discharge Machining.
10. Kinoshita, N., Fukui, M. and Fujii, T., 1987. Study on wire-EDM: accuracy in taper-cut. CIRP Annals-Manufacturing Technology, 36(1), pp.119-122.
11. Okada, A., Konishi, T., Okamoto, Y. and Kurihara, H., 2015. Wire breakage and deflection caused by nozzle jet flushing in wire EDM. CIRP Annals-Manufacturing Technology, 64(1), pp.233-236.
12. Scott, D., Boyina, S. and Rajurkar, K.P., 1991. Analysis and optimization of parameter combinations in wire electrical discharge machining. THE INTERNATIONAL JOURNAL OF PRODUCTION RESEARCH, 29(11), pp.2189-2207.
13. Nayak, B.B. and Mahapatra, S.S., 2014. A Utility Concept Approach for Multi-objective optimization of Taper Cutting Operation using WEDM. Procedia Engineering, 97, pp.469-478.

14. Rao, P.S., Ramji, K. and Satyanarayana, B., 2014. Experimental Investigation and Optimization of Wire EDM Parameters for Surface Roughness, MRR and White Layer in Machining of Aluminium Alloy. Procedia Materials Science, 5, pp.2197-2206.
15. Sarkar, S., Mitra, S., Gomes, I.K. and Bhattacharyya, B., 2005. Modeling and Optimization of Wire Electrical Discharge Machining In Single Pass Cutting Operation. In Proceedings of the International Conference on Mechanical Engineering, Dhaka, Bangladesh.
16. Bobbili, R., Madhu, V. and Gogia, A.K., 2015. Multi response optimization of wire-EDM process parameters of ballistic grade aluminium alloy. Engineering Science and Technology, an International Journal, 18(4), pp.720-726.
17. Saedon, J.B., Jaafar, N., Yahaya, M.A., Saad, N. and Kasim, M.S., 2014. Multi-objective optimization of titanium alloy through orthogonal array and grey relational analysis in WEDM. Procedia Technology, 15, pp.832-840.
18. Aravind, S.N., Sowmya, S. and Yuvaraj, K.P., 2012, March. Optimization of metal removal rate and surface roughness on wire EDM using Taguchi method. In Advances in Engineering, Science and Management (ICAESM), 2012 International Conference on (pp. 155-159). IEEE.
19. Takeyasu, K. and Kainosho, M., 2014. Optimization technique by genetic algorithms for international logistics. Journal of Intelligent Manufacturing, 25(5), pp.1043-1049.
20. Tilekar, S., Das, S.S. and Patowari, P.K., 2014. Process Parameter Optimization of Wire EDM on Aluminum and Mild Steel by Using Taguchi Method. Procedia Materials Science, 5, pp.2577-2584.
21. Plaza, S., Ortega, N., Sanchez, J.A., Pombo, I. and Mendikute, A., 2009. Original models for the prediction of angular error in wire-EDM taper-cutting. The International Journal of Advanced manufacturing Technology, 44(5-6), pp.529-538.
22. Sanchez, J.A., Plaza, S., Ortega, N., Marcos, M. and Albizuri, J., 2008. Experimental and numerical study of angular error in wire-EDM taper-cutting. International Journal of Machine Tools and Manufacture, 48(12), pp.1420-1428.
23. Hsue, A.W.J. and Su, H.C., 2004. Removal analysis of WEDM's tapering process and its application to generation of precise conjugate surface. Journal of materials processing technology, 149(1), pp.117-123.
24. Sanchez, J.A., Plaza, S., Lopez de Lacalle, L.N. and Lamikiz, A., 2006. Computer simulation of wire-EDM taper-cutting. International Journal of Computer Integrated Manufacturing, 19(7), pp.727-735.

25. Bobbili, R., Madhu, V. and Gogia, A.K., 2015. Modelling and analysis of material removal rate and surface roughness in wire-cut EDM of armour materials. Engineering Science and Technology, an International Journal, 18(4), pp.664-668.
26. Datta, S. and Mahapatra, S., 2010. Modeling, simulation and parametric optimization of wire EDM process using response surface methodology coupled with grey-Taguchi technique. International Journal of Engineering, Science and Technology, 2(5), pp.162-183.
27. Steve Bond, National Sales Manager, FANUC RoboDrill, RoboCut and EDM Products from Methods Machine Tools, Inc. Online [Available]: http://www.moldmakingtechnology.com/articles/soft-wired-cutting-high-taper-angles-with-wire-edm-